Relationship Prompt Learning is Enough for Open-Vocabulary Semantic Segmentation

Jiahao Li¹, Yang Lu^{1,2,3}, Yuan Xie*4,5 and Yanyun Qu*1,2,3

¹School of Informatics, Xiamen University
²Institute of Artificial Intelligence, Xiamen University
³Key Laboratory of Multimedia Trusted Perception and Efficient Computing, Ministry of Education of China, Xiamen University
⁴School of Computer Science and Technology, East China Normal University
⁵Chongqing Institute of East China Normal University

Abstract

Open-vocabulary semantic segmentation (OVSS) aims to segment unseen classes without corresponding labels. Existing Vision-Language Model (VLM)-based methods leverage VLM's rich knowledge to enhance additional explicit segmentation-specific networks, yielding competitive results, but at the cost of extensive training cost. To reduce the cost, we attempt to enable VLM to directly produce the segmentation results without any segmentation-specific networks. Prompt learning offers a direct and parameter-efficient approach, yet it falls short in guiding VLM for pixel-level visual classification. Therefore, we propose the Relationship Prompt Module (RPM), which generates the relationship prompt that directs VLM to extract pixel-level semantic embeddings suitable for OVSS. Moreover, RPM integrates with VLM to construct the Relationship Prompt Network (RPN), achieving OVSS without any segmentation-specific networks. RPN attains state-of-the-art performance with merely about 3M trainable parameters (2% of total parameters).

1 Introduction

Open-vocabulary semantic segmentation (OVSS) [1–4] aims to segment novel classes without corresponding training images, which is still a challenging task in computer vision. Vision-Language Model (VLM) [5–7] has emerged as a powerful approach, acquiring comprehensive knowledge via large-scale image-caption matching training. Several VLM-based OVSS methods [8–10] achieve promising results. These methods employ the rich image-text representation knowledge inherent in VLM to improve segmentation performance and are categorized into two types: two-stage and one-stage methods. Two-stage methods [11–14] first generate image-level masks without semantics via a well-designed mask proposal network [15–18] and then classify these masks via the image-level classification ability of VLM. One-stage methods [19, 20] employ a semantic decoding network to distill VLM's comprehensive knowledge from the image to the pixel level, thereby producing pixel-level segmentation results.

However, both of these VLM-based methods rely on additional explicit segmentation-specific networks to obtain segmentation results, resulting in extensive training cost. To reduce the training cost, an intuitive idea is to make VLM directly produce segmentation results without these segmentation-

74298

38th Conference on Neural Information Processing Systems (NeurIPS 2024).

^{*}Corresponding author: yxie@cs.ecnu.edu.cn, yyqu@xmu.edu.cn

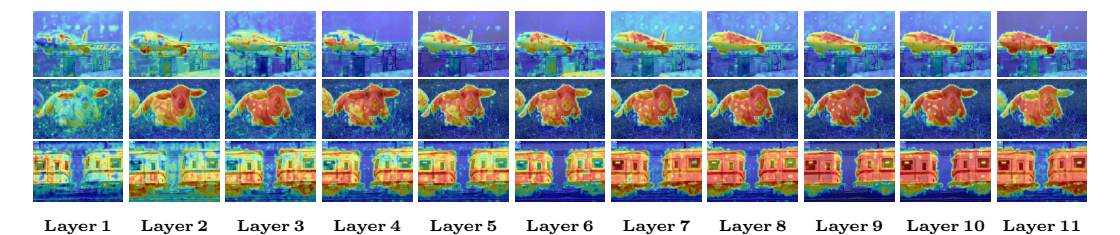


Figure 1: **Visualization of relationship attention map m from the well-trained RPN.** The degree of attention from low to high is marked by colors from dark blue to red. The more attention, the darker red; the less attention, the darker blue. As the layers deepen, the attention maps exhibit increasingly precise pixel-level semantics. The images correspond to the attention maps for an aeroplane, a sheep, and a train, respectively.

specific networks¹. In this context, prompt learning [5, 21–23] emerges as a practical approach, guiding VLM to transform image-text pair embeddings into pixel-level semantic embeddings suitable for OVSS, thereby directly achieving OVSS.

Without explicit segmentation-specific networks, applying prompt learning solely to VLM for OVSS is straightforward yet challenging. Typically, existing prompt learning methods fine-tune task-specific models to enhance performance on that task, yet they fail to secure cross-task performance gains. These methods employ either fixed or trainable vision prompt tokens [24], or they construct complex ViT-based networks for generating prompt [25, 26, 20, 27]. The limitations of such prompt include: 1) providing only image-level granularity, which restricts VLMs from performing tasks related to pixel-level visual classification, and 2) a lack of an image-text relationship, which hinders the exploration of VLMs' potential for open-vocabulary scene understanding. Therefore, it is difficult for these methods to enable VLM suitable for image-level classification to achieve open-vocabulary semantic segmentation directly.

In summary, addressing the above-mentioned issue lies in refining the granularity of prompt and strengthening the image-text relationship within them. By analyzing the outputs of VLM's encoder layer, we find they can construct an image-text relationship attention map via the attention mechanism, guiding the encoder to focus on relevant pixels. Thus, we propose the Relationship Prompt Module (RPM) that utilizes the outputs of image and text encoding layers to enable pixel-level relationship prompting, enhancing prompt's granularity and image-text relationship. Moreover, we

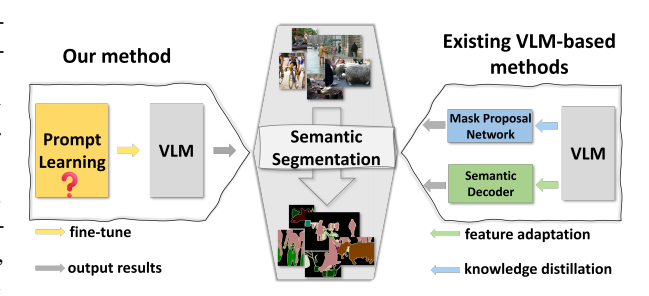


Figure 2: **Our method** *vs* **existing VLM-based methods.** Our method employs VLM to directly perform OVSS by prompt learning, while the other methods relies on additional explicit segmentation-specific networks.

implement a layer-by-layer guidance mode in VLM, enabling a progressive transfer of embeddings from the image to pixel level. As illustrated in Figure 1, each layer's relationship attention map is continuously refined following an image-to-pixel attention scheme. To obtain the segmentation results, we propose the Linear Projection Module (LPM) comprising merely two individual linear layers, which maps the image and text feature into a shared space, and then computes their Matrix product to produce the results. Finally, we propose the Relationship Prompt Network (RPN), which consists of RPM, LPM and VLM. Figure 2 shows the comparison between RPN and other OVSS methods. RPN employs VLM to directly output pixel-level predictions by prompt learning, while other methods use VLM to assist explicit segmentation-specific networks to obtain predictions. In these VLM-based methods, VLM transfers its rich knowledge to the mask proposal network by knowledge distillation or enables the semantic decoder to output segmentation masks by feature adaptation. The key difference between RPN and existing VLM-based methods is that RPN does

¹To achieve the idea, some works train the VLM from scratch using pixel-level supervision, which relies on large-scale pixel-level pre-training. Note that we aim to employ a parameter-efficient fine-tuning method to reduce the need for additional segmentation-specific networks and large-scale pre-training.

not require any explicit segmentation-specific networks; it only adapts VLM to perform OVSS. Our contributions are summarized as follows:

- We propose the Relationship Prompt Module (RPM), which generates pixel-level relationship prompt to guide VLM in transforming image-level embeddings to pixel-level ones suitable for OVSS.
- We propose the **R**elationship **P**rompt **N**etwork (**RPN**), employing prompt learning solely to adapt VLM for OVSS without explicit segmentation-specific networks.
- RPN attains state-of-the-art results on four public benchmarks by optimizing about **3M** trainable parameters (2% of total parameters).

2 Related Works

Open-Vocabulary Semantic Segmentation. Open-vocabulary semantic segmentation [28, 29] aims to leverage the knowledge from representation distributions of seen categories to classify unseen categories. Existing methods can be divided into two types: generative and discriminative. Generative methods [30, 31, 28, 32] require the segmentation network to be aware of which categories are unseen during training, while discriminative methods [11, 8, 19, 33] directly transfer semantics from seen to unseen categories, which is more straightforward. SPNet [33] introduces the zero-shot task for the first time and proposes an end-to-end training paradigm, in which the visual embeddings are composed with the uniform semantic word embeddings to obtain the semantic logits. ZS3Net [31] utilizes a generative approach to project the text embeddings into visual space and generate visual embeddings for unseen categories. Subsequently, many works following the generative method have been proposed. STRICT [34] assumes that the pixels of unseen categories can be present during training the model and adopts the self-training strategy to optimize the model for classifying the unseen categories. GaCNet [30] proposes a novel context-aware feature generation method based on ZS3Net, in which pixel-wise contextual knowledge can be utilized to guide the feature generation process of unseen categories. CLIP-based approaches have also made great progress. ZegFormer [11] proposes two sub-tasks, i.e., class-agnostic grouping and segment-level zero-shot classification and presents the CLIP-based method for the first time. MaskCLIP [8] utilizes the frozen CLIP to make a minimal adaptation by fine-tuning a lightweight classifier and replacing it with that of the segmentation network. Zsseg [12] proposes a two-stage CLIP-based method, in which a proposal generator is used to generate binary masks and CLIP is required to classify them. ZegCLIP [19] presents a one-stage method in which CLIP directly transfers knowledge to a lightweight decoder.

Vision-Language Models for Vision Tasks. Vision-language models for vision tasks [5, 21–23] are optimized with a large scale of image-text pair data on the internet. There are three categories: contrastive, generative, and aligned objectives. CLIP [5] first proposes the paradigm of pre-trained vision-language model. DeCLIP [35] argues that CLIP is data-intensive and proposes a data-efficient training paradigm. UniCL [36] combines the two data sources to build a new image-text-label field and proposes unified contrastive learning. ZeroVL [21] proposes debiased sampling to deal with biased representation distributions and a new mixup method for the image and text models. OTTER [22] uses optimal transport to find the soft label for contrastive learning and handle the problem of noisy image-text pairs.

Visual Prompt Learning. Visual Prompt Learning [37–39] is a technique that assists in adapting CLIP-like vision-language models for various visual tasks. CoOp [40] adopts trainable vectors as word prompt to adapt CLIP for vision classification. VP [41] utilizes perturbations as visual prompt. VPT [24] proposes trainable visual prompt to adapt each layer of the visual embeddings. UPT [38] constructs unified prompt modeling to extract trainable visual and textual prompt for adapting CLIP. MaPLe [39] adopts trainable prompt to guide both visual and textual embeddings and proposes a coupling function as a bridge to build a multi-modal prompt. DenseCLIP [26] uses the contextual information from the image to prompt the language model. Probabilistic prompt [20] applies multiple prompt sampled from probabilistic text embeddings to better understand the image. SegPrompt [27] proposes a category-level prompt to improve the model's class-agnostic segmentation ability.

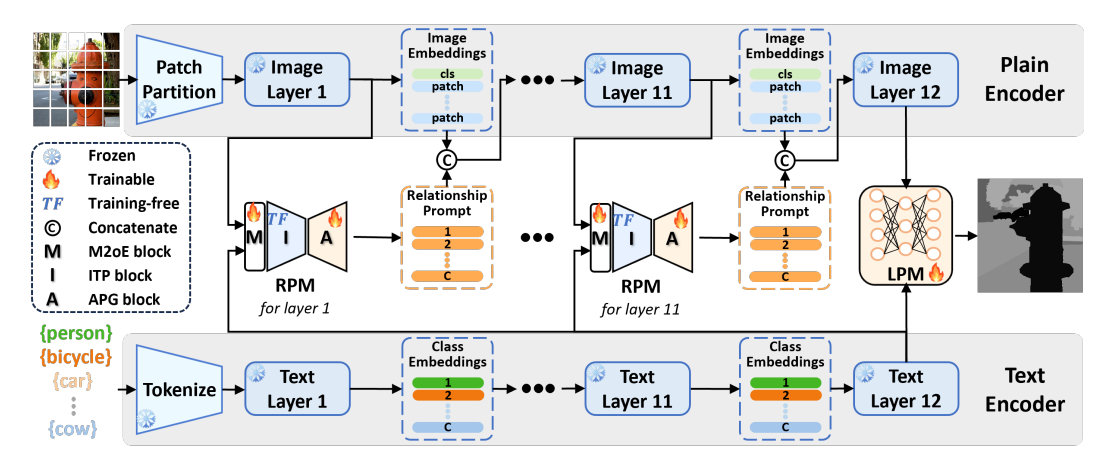


Figure 3: **Overview of RPN.** The end-to-end architecture is delineated into four principal components: 1) the frozen plain encoder, which adopts ViT architecture to encode visual knowledge with relationship prompt; 2) the frozen text encoder, which adopts CLIP text encoder architecture to encode class knowledge with text templates; 3) Relationship Prompt Module (RPM), which generates relationship prompt to guide the plain encoder to output pixel-level semantic embeddings; 4) Linear Projection Module (LPM), which consists of two individual linear layers to output OVSS results.

3 Approach

Overview. Our objective is to adopt prompt learning to develop a VLM-based OVSS method without any explicit segmentation-specific networks, thereby reducing training cost. As shown in Figure 3, the **Relationship Prompt Network** (**RPN**) is an end-to-end system comprising text, image and image-text relationship prompt branches. In the text branch, the text encoder inputs text to yield the class embeddings $\mathbf{t} \in \mathbb{R}^{C \times d}$, where C and d represent the number of classes and dimension, respectively. In the image branch, the plain encoder inputs images to obtain the image embeddings $\mathbf{v} \in \mathbb{R}^{(N+1)\times d}$, which includes the patch embeddings $\mathbf{p} \in \mathbb{R}^{N \times d}$ and the [CLS] token $\mathbf{g} \in \mathbb{R}^{1 \times d}$, with N representing the number of patches. Concurrently, in the image-text relationship prompt branch, the proposed **Relationship Prompt Module** (**RPM**) alongside the encoder takes the class and image embeddings to generate pixel-level relationship prompt, which is subsequently concatenated with the image embeddings to serve as the input for the next image layer. To obtain segmentation results, the last class and image embeddings are fed into the proposed **L**inear **P**rojection **M**odule (**LPM**) to calculate their Matrix product.

Relationship Prompt Module. RPM can guide the plain encoder of VLM to directly produce pixel-level semantic embeddings suitable for OVSS, due to its acquisition of three distinct types of knowledge. Firstly, it acquires multi-scale vision knowledge to locate objectives at distinct scales. Secondly, its image-text relationship knowledge enables the plain encoder to learn open-vocabulary semantics from text features. Thirdly, it introduces dynamic pixel-level knowledge, which is adaptive for the relationship knowledge, enabling pixel-level relationship prompt learning and thus transforming VLM's image-level embeddings into pixel-level ones. Therefore, RPM comprises three blocks, each dedicated to capturing one of the aforementioned knowledge types.

It is crucial for OVSS to obtain multiscale image embeddings to locate targets of different scales. However, the image embeddings maintain a consistent scale across each image layer. Therefore, we propose multi-scale mixture-of-experts (M2oE) block to aggregate the patch embeddings across distinct scales. As illustrated in Figure 4, M2oE comprises a gating network and several



Figure 4: **M2oE.** \otimes and \oplus denote matrix product and addition.

expert networks as in [42, 43]. The gating network aims to dynamically activate different experts, each responsible for scaling the input to various extents. M2oE of the i-th layer is formulated as follows:

$$\mathbf{p}^{i} \leftarrow \mathbf{p}^{i} + \sum_{j=1}^{n} G(\mathbf{p}^{i})_{j} \mathbf{Linear}_{\mathbf{r} \to \mathbf{d}}(E_{j}(\mathbf{p}^{i}))$$
 (1)

where $G(\cdot)$ and $E_j(\cdot)$ represent the gating network and the j-th expert of all n experts, respectively. Note that the patch embeddings first reduce the dimension from d to r=3. And $\mathbf{Linear}(\cdot)$ maps the output of each expert back to the original dimension d. See Appendix B for more details on M2oE.

It is crucial for OVSS to fuse the image embeddings with open-vocabulary semantics of the class embeddings. The key is to construct the image-text relationship that bridges the class and image embeddings. To achieve this, we propose image-to-pixel semantic attention (ITP) block, which utilizes the image embeddings and the last class embeddings to form the relationship attention map $\mathbf{m} \in \mathbb{R}^{N \times C}$. As illustrated in Figure 5, we first calculate the Hadamard product between the [CLS] token g and the last class embeddings t after dimension alignment. Then, the **Matrix product** between the Hadamard product result and the patch embeddings p yields the relationship attention map m. Consequently, the relationship attention map \mathbf{m}^i of the *i*-th layer is formulated as follows:

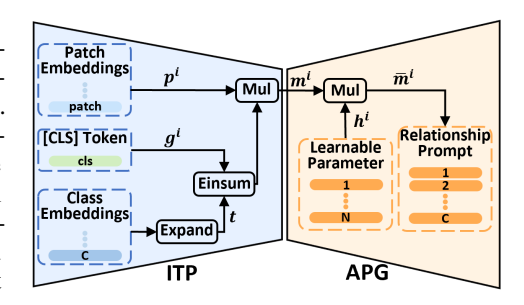


Figure 5: **ITP and APG.** Expand, Einsum and Mul denote expanding class dimension, Hadamard product and Matrix product.

$$\mathbf{m}^i = \mathbf{p}^i \cdot (t \odot \mathbf{g}^i)^\top \tag{2}$$

Intuitively, the first Hadamard product operation assigns weights to images in a batch, with their sum being one (the more important the image, the larger the weight), by fusing the class embeddings used to identify different classes and the [CLS] token used to identify each image in a batch, thus attaining image-level attention. The subsequent Matrix product operation weights the pixels, with the sum of pixel weights normalized to one (the more important the pixel, the larger the weight), by integrating the patch embeddings that contain pixel-level visual information, thus securing pixel-level attention. Therefore, we refer to the training-free operation (i.e., Eq. 2) as the image-to-pixel attention scheme, in which the first and the subsequent products extract image-level and pixel-level information, respectively. As illustrated in Figure 1, the relationship attention map construction process from the shallow to the deep layer demonstrates the effectiveness of the image-to-pixel attention scheme.

The construction of the adaptive image-text relationship for each pixel enables VLM to directly output pixel-level semantic embeddings. To achieve pixel-level dynamic tuning, we propose adaptive prompt generation (APG) block. As illustrated in Figure 5, we first initialize a trainable parameter $\mathbf{h} \in \mathbb{R}^{N \times d}$, representing the dynamic pixel-level knowledge. The adaptive relationship prompt $\bar{\mathbf{m}} \in \mathbb{R}^{C \times d}$ for each pixel is then derived from the Matrix product between the dynamic pixel-level knowledge \mathbf{h} and the relationship attention map \mathbf{m} . Consequently, the adaptive relationship prompt $\bar{\mathbf{m}}^i$ of the i-th layer is formulated as follows:

$$\bar{\mathbf{m}}^i = {\mathbf{m}^i}^\top \cdot \mathbf{h}^i \tag{3}$$

The role of the dynamic pixel-level knowledge h is twofold: 1) it projects the relationship attention map from a lower to a higher dimension to serve as an input for the plain encoder, 2) it fine-tunes the relationship prompt for each pixel. It is the fine-tuning of the relationship prompt for each pixel in a high-dimensional space that enables the plain encoder to directly obtain pixel-level semantics.

In addition, we integrate RPM in parallel within each layer of VLM. The image embeddings and the last class embeddings are fed into RPM to generate the relationship prompt, which is then merged with the image embeddings and fed into the next image layer. The prompt output from the image layer is discarded. The processing of each image layer is formulated as follows:

$$[\mathbf{v}^i, _] = \mathbf{Layer}^i([\mathbf{v}^{i-1}, \bar{\mathbf{m}}^{i-1}]) \tag{4}$$

The notation [,] represents the concatenation operation. See Appendix C for more details on RPM.

Linear Projection Module. Given that RPM enables the plain encoder to directly obtain pixel-level semantics, LPM aims to map the last image and class embeddings into a common space and calculate their Matrix product as the segmentation results. To this end, there are three intuitive designs as illustrated in Figure 6. All three designs share a common structure, consisting of an image branch and a text branch, each equipped with a linear layer and a normalization layer. The

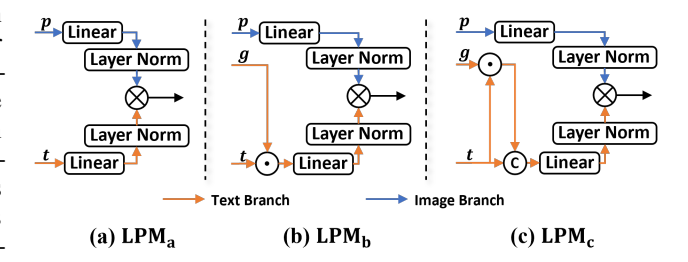


Figure 6: Three kinds of LPMs. \odot and \otimes denote elementwise product and matrix product.

image branch processing (the blue solid line) remains consistent, with the last patch embeddings p sequentially passing through the linear layer and the normalization layer. The difference lies in the text branch processing (the orange solid line). In LPM_a (as shown in Figure 6 (a)), only the last class embeddings t are factored into the text branch. In LPM_b (as shown in Figure 6 (b)), the last class embeddings t and the last [CLS] token g first produce the Hadamard product before entering into the linear layer. In LPM_c (as shown in Figure 6 (c)), the last class embeddings t is concatenated with the Hadamard product result and then fed into the linear layer. Thus, the segmentation results \mathbf{O}_a , \mathbf{O}_b and \mathbf{O}_c of them are defined as follows:

$$\mathbf{O}_a = \mathbf{Linear}(p) \cdot \mathbf{Linear}(t)^{\top} \tag{5}$$

$$\mathbf{O}_b = \mathbf{Linear}(p) \cdot \mathbf{Linear}(t \odot g)^{\top} \tag{6}$$

$$\mathbf{O}_c = \mathbf{Linear}(p) \cdot \mathbf{Linear}([t \odot g, t])^{\top}$$
(7)

For simplicity, the normalization layers are omitted. We select LPM_c as the proposed LPM experimentally (as shown in Table 6).

Optimization. There are two types of loss functions: the cross-entropy loss with the Softmax function and the combination loss between the focal loss and the dice loss with the Sigmoid function. The former employs one-hot encoding to render the class distribution as mutually exclusive in the embedding space, while the latter utilizes multi-label encoding to permit class distribution overlap. Practically, these losses are typically selected based on the used semantic decoders, such as the former with FPN[44] and the latter with a transformer decoder[45]. Considering that we employ LPM (comprising just two individual linear layers) to obtain the final segmentation results without any well-designed semantic decoders, we evaluate the aforementioned two loss functions. We refer to the former as the Softmax loss and the latter as the Sigmoid loss. We select the Sigmoid loss experimentally (as shown in Table 6).

The Softmax loss is formulated as follows:

$$\mathcal{L}_{softmax} = -\sum_{k=1}^{h \times w} y_k \cdot \log \hat{y}_k \tag{8}$$

where y_k and \hat{y}_k are the ground truth and the prediction vectors, respectively, and h and w represent the height and width of the input image. The Sigmoid loss is formulated as follows:

$$\mathcal{L}_{focal} = -\sum_{k=1}^{h \times w} \alpha \cdot (\mathbf{1} - \hat{y}_k)^{\gamma} \cdot y_k \cdot \log(\hat{y}_k)$$
(9)

$$\mathcal{L}_{dice} = 1 - \frac{2\sum_{k=1}^{h \times w} \hat{y}_k \cdot y_k^{\top}}{\sum_{k=1}^{h \times w} \hat{y}_k \cdot \hat{y}_k^{\top} + \sum_{k=1}^{h \times w} y_k \cdot y_k^{\top}}$$
(10)

$$\mathcal{L}_{sigmoid} = \lambda_1 \mathcal{L}_{focal} + \lambda_2 \mathcal{L}_{dice} \tag{11}$$

where α , γ , λ_1 and λ_2 are hyperparameters. In Eq. 9, when y_k equals the zero vector, y_k and \hat{y}_k are substituted with $1 - y_i$ and $1 - \hat{y}_i$, respectively.

4 Experiments

We evaluate our method in both zero-shot and open-vocabulary settings. See Appendix D for more details on the settings.

4.1 Implementation Details

Datasets and Evaluation Metrics. ADE20K[46] consists of 25k images for training and 2k images for validation. Pascal VOC 2012[47] includes 10,582 augmented training images and 1,449 validation images. COCOStuff164K[48] contains 118,287 training images and 5,000 validation images, with 171 classes in total. Pascal Context[49] consists of 10,100 images, of which 4,996 are used for training and 5,104 for validation, covering 60 classes. We employ pixel-wise

Table 1: Efficiency comparison with state-of-the-art methods. #Params(M) represents the total number of trainable parameters.

Methods	#Params(M)	FLOPs(G)	FPS
	VOC		
ZegFormer [11]	60.3	1829.3	1.7
ZegCLIP [19]	13.8	110.4	9.0
RPN(ours)	3.2	84.2	10.6
	COCO		
ZegFormer [11]	60.3	1875.1	1.5
ZegCLIP [19]	14.6	123.9	6.7
RPN(ours)	3.2	101.3	10.2

classification accuracy (pAcc) and the mean of class-wise intersection over union (mIoU) for seen classes (mIoU_u), unseen classes (mIoU_u), and their harmonic mean (hIoU).

Training Strategy. We conduct all experiments on eight NVIDIA GTX 3090 GPUs using the MMSegmentation tool [50]. If not specified, we employ the pre-trained CLIP ViT-B/16 model for both the plain encoder and the text encoder. We set the batch size of 4 for each GPU and set the input resolution to 512×512 pixels. The data augmentation strategy adheres to the default settings in MMSegmentation, which includes random image resizing with a short-side range of [256, 1024] and a crop size of 512×512 . The optimizer is AdamW, initialized with a learning rate of 2×10^{-5} and a weight decay of 1×10^{-2} . The learning rate follows a polynomial decay schedule with a power of 0.9. The number of iterations is set to 20K for the VOC dataset, 80K for the COCO dataset, and 40K for the Context dataset. We set λ_1 and λ_2 in Eq. 11 to 100 and 1, respectively.

4.2 System Level Comparison

Efficiency Comparison. We present an efficiency comparison with state-of-the-art methods in Table 1. The results of compared methods are derived from [19]. To ensure a fair comparison, we report our results based on the open-source code from [19] and evaluate them with an input resolution of 512×512 on a single NVIDIA GTX 1080 Ti GPU. Our method outperforms the other methods in efficiency, achieving the lowest number of trainable parameters and the smallest FLOPs.

Comparison in the Zero-Shot Setting. We show the performance comparison with the state-of-the-art methods in the zero-shot setting in Table 2, and conduct the comparison under three scenarios: without self-training, with self-training, and fully supervised. In the absence of self-training, our method surpasses FreeSeg [10] with +6.0% mIoU_u on the VOC dataset and +0.6% mIoU_u on the COCO dataset. With self-training, our method outperforms ZegCLIP [19] with +3.7% mIoU_u on the VOC dataset, +1.3% mIoU_u on the COCO dataset, and +2.3% mIoU_u on the Context dataset. Under the fully supervised scenario, our method exceeds ZegCLIP [19] with an average of +2.0% mIoU_u across the three datasets. We attribute the modest improvement on the COCO dataset to the bias from the extremely unbalanced training and validation set ratios (more training data and less validation data), which contrasts with the performance on the Context dataset (less training data and more validation data), reflecting the robust zero-shot learning ability of our method.

Comparison in the Open-Vocabulary Setting. We show the performance comparison with the state-of-the-art methods in the open-vocabulary setting in Table 3. Our method does not require an additional training dataset. The results indicate that no method can consistently outperform others across all validation datasets; however, our method attains state-of-the-art performance on the A-847, A-150 and the PAS-20 datasets. As analyzed in [53], the Context dataset and the ADE20K dataset

74304

Table 2: **Performance comparison in the zero-shot setting (unit:%).** Here, the best results are shown in bold and the second-best results are underlined. The self-training represents applying self-training via generating pseudo labels on all unlabeled pixels like in [19, 8]. The symbol '†' indicates pseudo labels are merely annotated on unseen classes pixels excluding the ignore part.

- M. d. 1		V(OC			CO	CO			Con	text		
Methods	pAcc	$mIoU_s$	\mathbf{mIoU}_u	hIoU	pAcc	$mIoU_s$	\mathbf{mIoU}_u	hIoU	pAcc	$mIoU_s$	\mathbf{mIoU}_u	hIoU	
w/o self-training													
ZegFormer [11]	-	86.4	63.6	73.3	-	36.6	33.2	34.8	-	-	-	-	
ZegFormer+MAFT [51]	-	91.5	80.7	85.7	-	36.4	40.1	38.1	-	-	-	-	
ZSSeg [12]	90.0	83.5	72.5	77.5	60.3	39.3	36.3	37.8	-	-	-	-	
ZSSeg +MAFT [51]	-	87.1	76.1	81.2	-	36.1	35.9	36.0	-	-	-	-	
ZegCLIP [19]	94.6	91.9	77.8	84.3	62.0	40.2	41.4	40.8	76.2	46.0	54.6	49.9	
FreeSeg [10]	-	91.9	78.6	84.7		42.4	42.2	42.3		_		-	
RPN(ours)	95.8	93.1	84.6	88.6	64.4	<u>40.8</u>	42.8	<u>41.8</u>	76.4	47.7	58.7	52.6	
				w/	self-tra	ining							
ZegCLIP [19]	95.1	91.8	82.2	86.7	68.8	40.6	54.8	46.6	77.2	46.6	65.4	54.4	
MaskCLIP† [8]	-	88.8	86.1	87.4	-	38.1	54.7	45.0	-	44.4	66.7	53.3	
ZegCLIP† [19]	96.2	92.3	89.9	91.1	69.2	40.7	59.9	48.5	77.3	46.8	68.5	55.6	
RPN†(ours)	97.1	93.1	93.6	93.3	69.3	<u>40.6</u>	61.2	48.8	78.3	48.1	70.8	57.3	
	fully supervised												
ZegCLIP [19]	96.3	92.4	90.9	91.6	69.9	40.7	63.2	49.6	77.5	<u>46.5</u>	78.7	56.9	
RPN(ours)	97.2	94.0	94.6	94.3	70.8	41.1	64.1	50.5	78.7	48.5	80.1	60.4	

Table 3: **Performance comparison in the open-vocabulary setting (unit:%).** Here, the best results are shown in bold and the second-best results are underlined.

Methods	VLM	Training Set	A-847	PC-459	A-150	PC-59	PAS-20
OVSeg [14]	ViT-B/16	COCO-Stuff+COCO Caption	7.1	11.0	24.8	53.3	92.6
CAT-Seg[52]	ViT-B/16	COCO-Stuff	8.4	16.6	27.2	57. 5	93.7
SAN[53]	ViT-B/16	COCO-Stuff	10.1	12.6	27.5	53.8	94.0
SED[54]	ConvNeXt-B	COCO-Stuff	11.4	18.6	31.6	<u>57.3</u>	94.4
RPN(ours)	ViT-B/16	COCO-Stuff	<u>11.4</u>	<u>17.3</u>	<u>31.5</u>	57.1	95.2
OVSeg [14]	ViT-L/14	COCO-Stuff+COCO Caption	9.0	12.4	29.6	55.7	94.5
CAT-Seg[52]	ViT-L/14	COCO-Stuff	10.8	20.4	31.5	62.0	96.6
SAN[53]	ViT-L/14	COCO-Stuff	13.7	17.1	33.3	60.2	95.5
FC-CLIP[55]	ConvNeXt-L	COCO Panoptic	14.8	18.2	34.1	58.4	95.4
SED[54]	ConvNeXt-L	COCO-Stuff	13.9	22.6	<u>35.2</u>	60.6	96.1
RPN(ours)	ViT-L/14	COCO-Stuff	14.9	<u>22.1</u>	36.4	<u>61.9</u>	<u>96.6</u>

exhibit the highest and lowest label-set similarities with the training dataset, respectively. Therefore, our method showcases a more comprehensive open-vocabulary learning ability.

4.3 Ablation Study

We conduct the ablation experiments on the VOC and the COCO datasets. If not specified, most are conducted on the VOC dataset. See Appendix D for more details on the experiments.

Image-to-Pixel Attention Scheme. RPM aims to transform image-level embeddings from VLM into pixel-level semantic embeddings, enabling direct OVSS. To illuminate its functionality, we employ the Mean Attention Distance (MAD) [56, 57] as a metric, reflecting the granularity of information aggregated within the self-attention head. As illustrated in Figure 7, we analyze MAD of each self-attention head during the initial and advanced stages of training. A higher point indicates a larger receptive field, and greater point spacing signifies richer feature diversity. In the initial training phase, shallow and deep layer information exhibit marked differences: the former concentrates on the local field with fine granularity and high diversity, while the latter focuses on the global field with coarse granularity and limited diversity. During training with RPM, deep layer information maintains attention on both local and global fields without sacrificing granularity or diversity. Clearly, deep layer information, augmented with relationship prompt learning, is more suitable for pixel-level semantic segmentation tasks, thereby diminishing the need for additional segmentation-specific networks. In addition, we visualize the relationship attention map in Figure 1. The first line denote the relationship attention maps for seen classes across each layer; the last two lines for unseen classes. For seen classes, the model has prior pixel-level semantic, so the relationship attention map only needs to focus on a few pixels to guide the model to make predictions for these pixels (e.g., the relationship attention map for airplane has fewer highlighted areas). For unseen classes, the model lacks corresponding semantic, so the relationship attention map needs to focus on more pixels to provide the model with

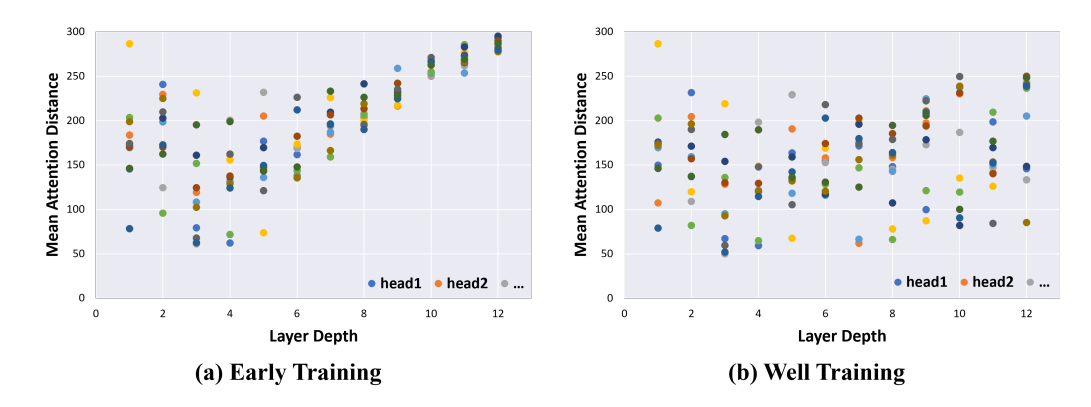


Figure 7: Mean Attention Distance of each self-attention head.

Table 4: **Impact of different modules (unit:%).** Methods without LPM represent eliminating the linear layers in LPM, i.e., discarding **Linear**(\cdot) in Eq.7.

	D3.f			T74	<u> </u>					
K	PM	LPM		VOC				CO	CO	
w/ M2oE	w/o M2oE	L/1 IV1	pAcc	\mathbf{mIoU}_s	\mathbf{mIoU}_u	hIoU	pAcc	\mathbf{mIoU}_s	\mathbf{mIoU}_u	hIoU
			77.1	76.3	14.3	24.1	48.3	31.8	16.4	21.6
	\checkmark		94.7	92.1	81.2	86.3	63.3	39.2	40.3	39.7
\checkmark			95.1	92.4	81.7	86.7	63.7	39.5	40.3	39.9
		\checkmark	88.8	87.3	45.3	59.6	49.3	31.3	20.3	24.6
	\checkmark	\checkmark	95.6	92.9	83.4	87.9	64.1	39.7	41.6	40.6
✓		\checkmark	95.8	93.1	84.6	88.6	64.4	40.8	42.8	41.8

more sufficient pixel-level semantic (e.g., the relationship attention map for sheep highlights the complete semantic at shallow layers).

Impact of Different Modules. Table 4 shows the impact of various modules. RPM (the first line) denotes the combination of M2oE, ITP and APG. RPM without M2oE (the second line) denotes the ablation about APG and ITP. Utilizing RPM and LPM yields the best performance. The performance improvement attributed to RPM (+62.6%) is significantly greater than that of LPM (+35.5%). Furthermore, integrating LPM on top of RPM yields a modest performance gain of 1.9%. In contrast, incorporating RPM based on LPM results in a substantial 29% improvement. Therefore, we conclude that VLM with relationship prompt learning is enough for OVSS without any explicit segmentation-specific networks.

Exploration of Different Designs in RPM. Firstly, we explore various designs of the ITP block. As discussed in Section 3, removing the patch embeddings, which contain pixel-level visual information, results in a loss of pixel-level attention for ITP. Conversely, omitting the [CLS] token, responsible for identifying each image, results in a loss of imagelevel attention. To assess the significance of the image-to-pixel attention scheme, we define the 'without pixel-level attention' and the 'without image-level attention' scenarios by excluding the patch embeddings \mathbf{p}^{i} and the [CLS] token g^i from Eq. 2, respectively. Note that employing the 'without pixel-level attention' scenario necessitates altering the dimension of

Table 5: Ablation study on different designs in RPM (unit:%).

	Attention	pAcc	\mathbf{mIoU}_s	\mathbf{mIoU}_u	hIoU
ITP	w/o image-level	73.1	74.2	21.4	33.2
111	w/o pixel-level	87.7	77.6	68.1	72.5
	w/ both	95.8	93.1	84.6	88.6
	Modes	pAcc	$mIoU_s$	\mathbf{mIoU}_u	hIoU
APG	nn.Linear	95.1	92.1	80.6	86.0
	nn.Parameter	95.8	93.1	84.6	88.6
	Dimension	pAcc	\mathbf{mIoU}_s	\mathbf{mIoU}_u	hIoU
	r=3	95.8	93.1	84.6	88.6
	r = 6	95.8	93.4	84.5	88.7
M2oE	r = 12	95.9	93.8	84.3	88.8
	Modes	pAcc	$mIoU_s$	\mathbf{mIoU}_u	hIoU
	Multi-Scale	94.9	92.8	84.1	88.2
	M2oE	95.8	93.1	84.6	88.6

the trainable parameter \mathbf{h}^i from $\mathbb{R}^{N\times d}$ to $\mathbb{R}^{d\times d}$. The results presented in Table 5 (ITP) corroborate the efficacy of the image-to-pixel attention scheme. Secondly, we explore different configurations of the APG block and evaluate two distinct trainable modes: nn.Linear and nn.Parameter. The outcomes in Table 5 (APG) advocate for the implementation of the nn.Parameter mode. Thirdly, we explore the dimension r of M2oE and different multi-scale aggregation modes in Table 5 (M2oE). The results show that performance enhancements are marginal with increasing dimensions. Given the trade-off between performance gain and parameter increase, we adopt r=3. The 'Multi-Scale' mode refers to removing the gating network and directly aggregating the features processed by all expert networks (See Appendix B for more details).

Exploration of Different Designs in LPM. We evaluate three different LPM designs (shown in Figure 6) using Softmax and Sigmoid losses. The results in Table 6 reveal that LPM_c with Sigmoid loss is the most effective strategy. In addition, using Sigmoid loss is significantly better than using Softmax loss. This reflects that the relationship prompt does not directly focus on pixels, but follows the image-to-pixel process.

Impact of Training-Free Projection Modules. Note that our method comprises two trainable modules: RPM and LPM. To further explore the performance of RPM, we eliminate all linear layers in LPM to construct three variants of training-free projection.

Table 6: Ablation study on three different LPMs using Softmax and Sigmoid losses (unit: %).

$\overline{\text{LPM}_a}$	\mathbf{LPM}_b	\mathbf{LPM}_c	pAcc	$mIoU_s$	\mathbf{mIoU}_u	hIoU					
Using Softmax loss											
$\overline{\hspace{1em}}$			70.6	67.3	19.6	30.3					
	\checkmark		89.4	88.6	55.5	68.2					
		✓	90.4	89.5	59.3	71.4					
		Using	Sigmoi	ld loss							
$\overline{}$			87.5	84.6	61.4	71.2					
	\checkmark		95.3	93.1	83.6	88.1					
		✓	95.8	93.1	84.6	88.6					

Table 7: Ablation study on three different training-free projection modules (unit: %).

$TFPM_a$	\mathbf{TFPM}_b	$TFPM_c$	pAcc	$mIoU_s$	\mathbf{mIoU}_u	hIoU
√			86.8	83.5	58.7	68.9
	\checkmark		94.5	92.4	77.6	84.4
		✓	95.1	92.4	81.7	86.7

tion networks. Following the sequence depicted in Figure 6, we denote the training-free projection modules as $TFPM_a$, $TFPM_b$ and $TFPM_c$. The results in Table 7 demonstrate that both $TFPM_b$ and $TFPM_c$ can achieve the state-of-the-art performance. The suboptimal results with $TFPM_a$ suggests that the relationship prompt guides the plain encoder to perform pixel-level classifications by encoding semantics in the [CLS] token, which should not be disregarded when obtaining segmentation results.

5 Conclusion

In this work, we propose the Relationship Prompt Module (RPM) to guide VLM to transform its image-level embeddings into pixel-level semantic ones. RPM and VLM combine to form Relationship Prompt Network (RPN), a VLM-based OVSS method that directly performs OVSS without any explicit segmentation-specific networks. To the best of our knowledge, we are the first to give a straightforward solution for OVSS that applies prompt learning solely to VLM. We evaluate our method on four public benchmark datasets in both zero-shot and open-vocabulary settings, and achieve the state-of-the-art performance with only about 3M trainable parameters (2% of total parameters). Therefore, it is concluded that VLM with relationship prompt learning is enough for open-vocabulary semantic segmentation without any explicit segmentation-specific networks.

Limitations. Although we meticulously design an effective prompt learning method for directly using VLM to achieve pixel-level OVSS, there are several ways for prompt learning to achieve further improvement: 1) directly acting on the attention map (more direct); 2) dynamically reorganizing multi-head attention map (more lightweight).

Acknowledgements.

This work is supported by the National Natural Science Foundation of China (No. 62176224, 62176092, 62222602, 62306165, 62106075, 62476090, 62376233, 62431004); Natural Science Foundation of Shanghai (23ZR1420400); Natural Science Foundation of Chongqing (NO.CSTB2023NSCQ-JQX0007); Natural Science Foundation of Fujian Province under Grant 2024J09001; China Computer Federation (CCF) Lenovo Blue Ocean Research Fund; China Academy of Railway Sciences No.2023YJ357; Xiaomi Young Talents Program.

References

- [1] Shuting He, Henghui Ding, and Wei Jiang. Primitive generation and semantic-related alignment for universal zero-shot segmentation. In *Proceedings of the IEEE/CVF Conference on Computer Vision and Pattern Recognition*, pages 11238–11247, 2023.
- [2] Hang Zhao, Xavier Puig, Bolei Zhou, Sanja Fidler, and Antonio Torralba. Open vocabulary scene parsing. In *Proceedings of the IEEE International Conference on Computer Vision*, pages 2002–2010, 2017.
- [3] Peike Li, Yunchao Wei, and Yi Yang. Consistent structural relation learning for zero-shot segmentation. *Advances in Neural Information Processing Systems*, 33:10317–10327, 2020.
- [4] Feihong Shen, Jun Liu, and Ping Hu. Conterfactual generative zero-shot semantic segmentation. *arXiv* preprint arXiv:2106.06360, 2021.
- [5] Alec Radford, Jong Wook Kim, Chris Hallacy, Aditya Ramesh, Gabriel Goh, Sandhini Agarwal, Girish Sastry, Amanda Askell, Pamela Mishkin, Jack Clark, et al. Learning transferable visual models from natural language supervision. In *International conference on Machine Learning*, pages 8748–8763. PMLR, 2021.
- [6] Chao Jia, Yinfei Yang, Ye Xia, Yi-Ting Chen, Zarana Parekh, Hieu Pham, Quoc Le, Yun-Hsuan Sung, Zhen Li, and Tom Duerig. Scaling up visual and vision-language representation learning with noisy text supervision. In *International conference on machine learning*, pages 4904–4916. PMLR, 2021.
- [7] Amanpreet Singh, Ronghang Hu, Vedanuj Goswami, Guillaume Couairon, Wojciech Galuba, Marcus Rohrbach, and Douwe Kiela. Flava: A foundational language and vision alignment model. In *Proceedings of the IEEE/CVF Conference on Computer Vision and Pattern Recognition*, pages 15638–15650, 2022.
- [8] Chong Zhou, Chen Change Loy, and Bo Dai. Extract free dense labels from clip. In *European Conference on Computer Vision*, pages 696–712. Springer, 2022.
- [9] Xinyu Liu, Beiwen Tian, Zhen Wang, Rui Wang, Kehua Sheng, Bo Zhang, Hao Zhao, and Guyue Zhou. Delving into shape-aware zero-shot semantic segmentation. In *Proceedings of the IEEE/CVF Conference on Computer Vision and Pattern Recognition*, pages 2999–3009, 2023.
- [10] Jie Qin, Jie Wu, Pengxiang Yan, Ming Li, Ren Yuxi, Xuefeng Xiao, Yitong Wang, Rui Wang, Shilei Wen, Xin Pan, et al. Freeseg: Unified, universal and open-vocabulary image segmentation. In *Proceedings of the IEEE/CVF Conference on Computer Vision and Pattern Recognition*, pages 19446–19455, 2023.
- [11] Jian Ding, Nan Xue, Gui-Song Xia, and Dengxin Dai. Decoupling zero-shot semantic segmentation. In Proceedings of the IEEE/CVF Conference on Computer Vision and Pattern Recognition, pages 11583– 11592, 2022.
- [12] Mengde Xu, Zheng Zhang, Fangyun Wei, Yutong Lin, Yue Cao, Han Hu, and Xiang Bai. A simple baseline for open-vocabulary semantic segmentation with pre-trained vision-language model. In *European Conference on Computer Vision*, pages 736–753. Springer, 2022.
- [13] Seonghoon Yu, Paul Hongsuck Seo, and Jeany Son. Zero-shot referring image segmentation with global-local context features. In *Proceedings of the IEEE/CVF Conference on Computer Vision and Pattern Recognition*, pages 19456–19465, 2023.
- [14] Feng Liang, Bichen Wu, Xiaoliang Dai, Kunpeng Li, Yinan Zhao, Hang Zhang, Peizhao Zhang, Peter Vajda, and Diana Marculescu. Open-vocabulary semantic segmentation with mask-adapted clip. In Proceedings of the IEEE/CVF Conference on Computer Vision and Pattern Recognition, pages 7061–7070, 2023.
- [15] Liang-Chieh Chen, Yukun Zhu, George Papandreou, Florian Schroff, and Hartwig Adam. Encoder-decoder with atrous separable convolution for semantic image segmentation. In *Proceedings of the European* conference on computer vision (ECCV), pages 801–818, 2018.
- [16] Changqian Yu, Jingbo Wang, Changxin Gao, Gang Yu, Chunhua Shen, and Nong Sang. Context prior for scene segmentation. In *Proceedings of the IEEE/CVF Conference on Computer Vision and Pattern Recognition*, pages 12416–12425, 2020.
- [17] Wenwei Zhang, Jiangmiao Pang, Kai Chen, and Chen Change Loy. K-net: Towards unified image segmentation. *Advances in Neural Information Processing Systems*, 34:10326–10338, 2021.
- [18] Bowen Zhang, Zhi Tian, Quan Tang, Xiangxiang Chu, Xiaolin Wei, Chunhua Shen, et al. Segvit: Semantic segmentation with plain vision transformers. Advances in Neural Information Processing Systems, 35:4971– 4982, 2022.

- [19] Ziqin Zhou, Yinjie Lei, Bowen Zhang, Lingqiao Liu, and Yifan Liu. Zegelip: Towards adapting clip for zero-shot semantic segmentation. In *Proceedings of the IEEE/CVF Conference on Computer Vision and Pattern Recognition*, pages 11175–11185, 2023.
- [20] Hyeongjun Kwon, Taeyong Song, Somi Jeong, Jin Kim, Jinhyun Jang, and Kwanghoon Sohn. Probabilistic prompt learning for dense prediction. In *Proceedings of the IEEE/CVF Conference on Computer Vision* and Pattern Recognition, pages 6768–6777, 2023.
- [21] Quan Cui, Boyan Zhou, Yu Guo, Weidong Yin, Hao Wu, Osamu Yoshie, and Yubo Chen. Contrastive vision-language pre-training with limited resources. In *European Conference on Computer Vision*, pages 236–253. Springer, 2022.
- [22] Bichen Wu, Ruizhe Cheng, Peizhao Zhang, Peter Vajda, and Joseph E Gonzalez. Data efficient languagesupervised zero-shot recognition with optimal transport distillation. arXiv preprint arXiv:2112.09445, 2021.
- [23] Timo Lüddecke and Alexander Ecker. Image segmentation using text and image prompts. In Proceedings of the IEEE/CVF Conference on Computer Vision and Pattern Recognition, pages 7086–7096, 2022.
- [24] Menglin Jia, Luming Tang, Bor-Chun Chen, Claire Cardie, Serge Belongie, Bharath Hariharan, and Ser-Nam Lim. Visual prompt tuning. In *European Conference on Computer Vision*, pages 709–727. Springer, 2022.
- [25] Lingbo Liu, Jianlong Chang, Bruce XB Yu, Liang Lin, Qi Tian, and Chang-Wen Chen. Prompt-matched semantic segmentation. arXiv preprint arXiv:2208.10159, 2022.
- [26] Yongming Rao, Wenliang Zhao, Guangyi Chen, Yansong Tang, Zheng Zhu, Guan Huang, Jie Zhou, and Jiwen Lu. Denseclip: Language-guided dense prediction with context-aware prompting. In *Proceedings of the IEEE/CVF Conference on Computer Vision and Pattern Recognition*, pages 18082–18091, 2022.
- [27] Muzhi Zhu, Hengtao Li, Hao Chen, Chengxiang Fan, Weian Mao, Chenchen Jing, Yifan Liu, and Chunhua Shen. Segprompt: Boosting open-world segmentation via category-level prompt learning. In *Proceedings* of the IEEE/CVF International Conference on Computer Vision, pages 999–1008, 2023.
- [28] Jiaxin Cheng, Soumyaroop Nandi, Prem Natarajan, and Wael Abd-Almageed. Sign: Spatial-information incorporated generative network for generalized zero-shot semantic segmentation. In *Proceedings of the IEEE/CVF International Conference on Computer Vision*, pages 9556–9566, 2021.
- [29] Donghyeon Baek, Youngmin Oh, and Bumsub Ham. Exploiting a joint embedding space for generalized zero-shot semantic segmentation. In *Proceedings of the IEEE/CVF International Conference on Computer Vision*, pages 9536–9545, 2021.
- [30] Zhangxuan Gu, Siyuan Zhou, Li Niu, Zihan Zhao, and Liqing Zhang. Context-aware feature generation for zero-shot semantic segmentation. In *Proceedings of the 28th ACM International Conference on Multimedia*, pages 1921–1929, 2020.
- [31] Maxime Bucher, Tuan-Hung Vu, Matthieu Cord, and Patrick Pérez. Zero-shot semantic segmentation. Advances in Neural Information Processing Systems, 32, 2019.
- [32] Weijia Wu, Yuzhong Zhao, Mike Zheng Shou, Hong Zhou, and Chunhua Shen. Diffumask: Synthesizing images with pixel-level annotations for semantic segmentation using diffusion models. *arXiv preprint arXiv:2303.11681*, 2023.
- [33] Yongqin Xian, Subhabrata Choudhury, Yang He, Bernt Schiele, and Zeynep Akata. Semantic projection network for zero-and few-label semantic segmentation. In *Proceedings of the IEEE/CVF Conference on Computer Vision and Pattern Recognition*, pages 8256–8265, 2019.
- [34] Giuseppe Pastore, Fabio Cermelli, Yongqin Xian, Massimiliano Mancini, Zeynep Akata, and Barbara Caputo. A closer look at self-training for zero-label semantic segmentation. In *Proceedings of the IEEE/CVF Conference on Computer Vision and Pattern Recognition*, pages 2693–2702, 2021.
- [35] Yangguang Li, Feng Liang, Lichen Zhao, Yufeng Cui, Wanli Ouyang, Jing Shao, Fengwei Yu, and Junjie Yan. Supervision exists everywhere: A data efficient contrastive language-image pre-training paradigm. arXiv preprint arXiv:2110.05208, 2021.
- [36] Jianwei Yang, Chunyuan Li, Pengchuan Zhang, Bin Xiao, Ce Liu, Lu Yuan, and Jianfeng Gao. Unified contrastive learning in image-text-label space. In *Proceedings of the IEEE/CVF Conference on Computer Vision and Pattern Recognition*, pages 19163–19173, 2022.

- [37] Kaiyang Zhou, Jingkang Yang, Chen Change Loy, and Ziwei Liu. Conditional prompt learning for vision-language models. In Proceedings of the IEEE/CVF Conference on Computer Vision and Pattern Recognition, pages 16816–16825, 2022.
- [38] Yuhang Zang, Wei Li, Kaiyang Zhou, Chen Huang, and Chen Change Loy. Unified vision and language prompt learning. *arXiv preprint arXiv:2210.07225*, 2022.
- [39] Muhammad Uzair Khattak, Hanoona Rasheed, Muhammad Maaz, Salman Khan, and Fahad Shahbaz Khan. Maple: Multi-modal prompt learning. In *Proceedings of the IEEE/CVF Conference on Computer Vision and Pattern Recognition*, pages 19113–19122, 2023.
- [40] Kaiyang Zhou, Jingkang Yang, Chen Change Loy, and Ziwei Liu. Learning to prompt for vision-language models. *International Journal of Computer Vision*, 130(9):2337–2348, 2022.
- [41] Hyojin Bahng, Ali Jahanian, Swami Sankaranarayanan, and Phillip Isola. Exploring visual prompts for adapting large-scale models. arXiv preprint arXiv:2203.17274, 2022.
- [42] Zihan Zhong, Zhiqiang Tang, Tong He, Haoyang Fang, and Chun Yuan. Convolution meets lora: Parameter efficient finetuning for segment anything model. *arXiv preprint arXiv:2401.17868*, 2024.
- [43] Noam Shazeer, Azalia Mirhoseini, Krzysztof Maziarz, Andy Davis, Quoc Le, Geoffrey Hinton, and Jeff Dean. Outrageously large neural networks: The sparsely-gated mixture-of-experts layer. *arXiv* preprint *arXiv*:1701.06538, 2017.
- [44] Tsung-Yi Lin, Piotr Dollár, Ross Girshick, Kaiming He, Bharath Hariharan, and Serge Belongie. Feature pyramid networks for object detection. In *Proceedings of the IEEE conference on computer vision and* pattern recognition, pages 2117–2125, 2017.
- [45] Bowen Cheng, Alex Schwing, and Alexander Kirillov. Per-pixel classification is not all you need for semantic segmentation. Advances in Neural Information Processing Systems, 34:17864–17875, 2021.
- [46] Bolei Zhou, Hang Zhao, Xavier Puig, Tete Xiao, Sanja Fidler, Adela Barriuso, and Antonio Torralba. Semantic understanding of scenes through the ade20k dataset. *International Journal of Computer Vision*, 127:302–321, 2019.
- [47] M. Everingham, L. Van Gool, C. K. I. Williams, J. Winn, and A. Zisserman. The PASCAL Visual Object Classes Challenge 2012 (VOC2012) Results. http://www.pascalnetwork.org/challenges/VOC/voc2012/workshop/index.html.
- [48] Holger Caesar, Jasper Uijlings, and Vittorio Ferrari. Coco-stuff: Thing and stuff classes in context. In Computer Vision and Pattern Recognition (CVPR), 2018 IEEE conference on. IEEE, 2018.
- [49] Roozbeh Mottaghi, Xianjie Chen, Xiaobai Liu, Nam-Gyu Cho, Seong-Whan Lee, Sanja Fidler, Raquel Urtasun, and Alan Yuille. The role of context for object detection and semantic segmentation in the wild. In *IEEE Conference on Computer Vision and Pattern Recognition (CVPR)*, 2014.
- [50] MMSegmentation Contributors. MMSegmentation: Openmmlab semantic segmentation toolbox and benchmark. https://github.com/open-mmlab/mmsegmentation, 2020.
- [51] Siyu Jiao, Yunchao Wei, Yaowei Wang, Yao Zhao, and Humphrey Shi. Learning mask-aware clip representations for zero-shot segmentation. Advances in Neural Information Processing Systems, 36:35631– 35653, 2023.
- [52] Seokju Cho, Heeseong Shin, Sunghwan Hong, Seungjun An, Seungjun Lee, Anurag Arnab, Paul Hongsuck Seo, and Seungryong Kim. Cat-seg: Cost aggregation for open-vocabulary semantic segmentation. arXiv preprint arXiv:2303.11797, 2023.
- [53] Mengde Xu, Zheng Zhang, Fangyun Wei, Han Hu, and Xiang Bai. Side adapter network for open-vocabulary semantic segmentation. In Proceedings of the IEEE/CVF Conference on Computer Vision and Pattern Recognition, pages 2945–2954, 2023.
- [54] Bin Xie, Jiale Cao, Jin Xie, Fahad Shahbaz Khan, and Yanwei Pang. Sed: A simple encoder-decoder for open-vocabulary semantic segmentation. *arXiv preprint arXiv:2311.15537*, 2023.
- [55] Qihang Yu, Ju He, Xueqing Deng, Xiaohui Shen, and Liang-Chieh Chen. Convolutions die hard: Open-vocabulary segmentation with single frozen convolutional clip. Advances in Neural Information Processing Systems, 36, 2024.

- [56] Alexey Dosovitskiy, Lucas Beyer, Alexander Kolesnikov, Dirk Weissenborn, Xiaohua Zhai, Thomas Unterthiner, Mostafa Dehghani, Matthias Minderer, Georg Heigold, Sylvain Gelly, et al. An image is worth 16x16 words: Transformers for image recognition at scale. arXiv preprint arXiv:2010.11929, 2020.
- [57] Maithra Raghu, Thomas Unterthiner, Simon Kornblith, Chiyuan Zhang, and Alexey Dosovitskiy. Do vision transformers see like convolutional neural networks? *Advances in neural information processing* systems, 34:12116–12128, 2021.
- [58] Edward J Hu, Yelong Shen, Phillip Wallis, Zeyuan Allen-Zhu, Yuanzhi Li, Shean Wang, Lu Wang, and Weizhu Chen. Lora: Low-rank adaptation of large language models. arXiv preprint arXiv:2106.09685, 2021.
- [59] Boyi Li, Kilian Q Weinberger, Serge Belongie, Vladlen Koltun, and René Ranftl. Language-driven semantic segmentation. arXiv preprint arXiv:2201.03546, 2022.
- [60] Golnaz Ghiasi, Xiuye Gu, Yin Cui, and Tsung-Yi Lin. Scaling open-vocabulary image segmentation with image-level labels. In European Conference on Computer Vision, pages 540–557. Springer, 2022.
- [61] Kunyang Han, Yong Liu, Jun Hao Liew, Henghui Ding, Jiajun Liu, Yitong Wang, Yansong Tang, Yujiu Yang, Jiashi Feng, Yao Zhao, et al. Global knowledge calibration for fast open-vocabulary segmentation. In Proceedings of the IEEE/CVF International Conference on Computer Vision, pages 797–807, 2023.
- [62] Alexander Kirillov, Kaiming He, Ross Girshick, Carsten Rother, and Piotr Dollár. Panoptic segmentation. In Proceedings of the IEEE/CVF conference on computer vision and pattern recognition, pages 9404–9413, 2019.
- [63] Jiarui Xu, Shalini De Mello, Sifei Liu, Wonmin Byeon, Thomas Breuel, Jan Kautz, and Xiaolong Wang. Groupvit: Semantic segmentation emerges from text supervision. In *Proceedings of the IEEE/CVF Conference on Computer Vision and Pattern Recognition*, pages 18134–18144, 2022.
- [64] Piyush Sharma, Nan Ding, Sebastian Goodman, and Radu Soricut. Conceptual captions: A cleaned, hypernymed, image alt-text dataset for automatic image captioning. In *Proceedings of the 56th Annual Meeting of the Association for Computational Linguistics (Volume 1: Long Papers)*, pages 2556–2565, 2018.
- [65] Bart Thomee, David A Shamma, Gerald Friedland, Benjamin Elizalde, Karl Ni, Douglas Poland, Damian Borth, and Li-Jia Li. Yfcc100m: The new data in multimedia research. *Communications of the ACM*, 59(2):64–73, 2016.
- [66] Jordi Pont-Tuset, Jasper Uijlings, Soravit Changpinyo, Radu Soricut, and Vittorio Ferrari. Connecting vision and language with localized narratives. In Computer Vision–ECCV 2020: 16th European Conference, Glasgow, UK, August 23–28, 2020, Proceedings, Part V 16, pages 647–664. Springer, 2020.
- [67] Zheng Ding, Jieke Wang, and Zhuowen Tu. Open-vocabulary panoptic segmentation maskclip. 2022.
- [68] Jiarui Xu, Sifei Liu, Arash Vahdat, Wonmin Byeon, Xiaolong Wang, and Shalini De Mello. Open-vocabulary panoptic segmentation with text-to-image diffusion models. In *Proceedings of the IEEE/CVF Conference on Computer Vision and Pattern Recognition*, pages 2955–2966, 2023.
- [69] Xudong Wang, Shufan Li, Konstantinos Kallidromitis, Yusuke Kato, Kazuki Kozuka, and Trevor Darrell. Hierarchical open-vocabulary universal image segmentation. Advances in Neural Information Processing Systems, 36, 2024.
- [70] Elad Ben Zaken, Shauli Ravfogel, and Yoav Goldberg. Bitfit: Simple parameter-efficient fine-tuning for transformer-based masked language-models. *arXiv preprint arXiv:2106.10199*, 2021.
- [71] Neil Houlsby, Andrei Giurgiu, Stanislaw Jastrzebski, Bruna Morrone, Quentin De Laroussilhe, Andrea Gesmundo, Mona Attariyan, and Sylvain Gelly. Parameter-efficient transfer learning for nlp. In *International conference on machine learning*, pages 2790–2799. PMLR, 2019.
- [72] Yi-Lin Sung, Jaemin Cho, and Mohit Bansal. Lst: Ladder side-tuning for parameter and memory efficient transfer learning. *Advances in Neural Information Processing Systems*, 35:12991–13005, 2022.
- [73] Dongze Lian, Daquan Zhou, Jiashi Feng, and Xinchao Wang. Scaling & shifting your features: A new baseline for efficient model tuning. Advances in Neural Information Processing Systems, 35:109–123, 2022.
- [74] Kaiming He, Xinlei Chen, Saining Xie, Yanghao Li, Piotr Dollár, and Ross Girshick. Masked autoencoders are scalable vision learners. In *Proceedings of the IEEE/CVF conference on computer vision and pattern* recognition, pages 16000–16009, 2022.

Appendix

A Our Structure vs Existing Structures

We show the comparison of our method and the existing VLM-based methods in Figure 8. In our method, we abandon the explicit segmentation-specific networks, i.e., the mask proposal network and the semantic decoder and guide VLM to directly output the segmentation results. In existing VLM-based methods, the entire OVSS framework consists of VLM, the mask proposal network and the semantic decoder, incurring extensive training cost. As illustrated in Section 1, the two-stage methods usually adopt knowledge distillation to transfer zero-shot learning ability to the segmentation-specific network, and the one-stage methods utilize feature adaptation to train the semantic decoder. In summary, prompt learning acts as the engine to drive VLM to directly achieve OVSS in our method. Conversely, in the existing VLM-based methods, VLM acts as the engine to drive the segmentation-specific network to indirectly achieve OVSS. Therefore, our method is more straightforward and more parameter-efficient.

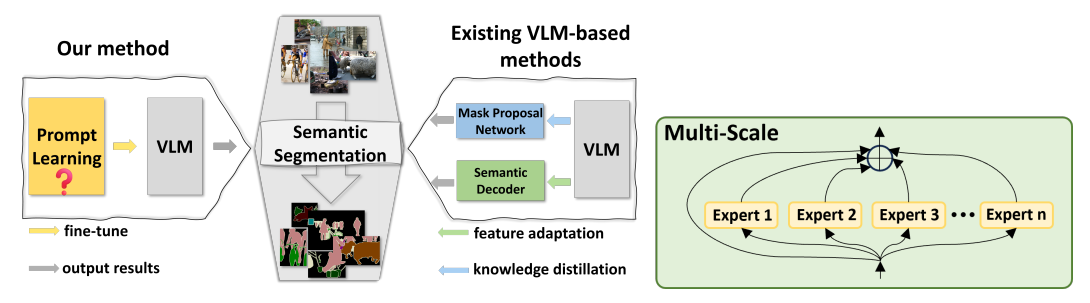


Figure 8: Our method vs existing VLM-based methods.

Figure 9: Multi-Scale.

B M2oE

Details The role of the gating network is to select the right expert for each sample in a batch. Thus, we need to calculate the gating scores $G(x) \in \mathbb{R}^{B \times n}$, i.e., the scores for B samples in a batch to n experts. For simplicity, let the input, i.e., the patch embeddings \mathbf{p} , be denoted by $x \in \mathbb{R}^{B \times N \times d}$, where $N = h \times w$. The input x is first directed into a common linear to reduce the dimension d to r, and then is reshaped to the size of $\mathbb{R}^{B \times r}$ after global average pooling (as Eq. 12). Like in [42, 43], the value $H(x) \in \mathbb{R}^{B \times n}$ is calculated as follows:

$$x_a = \text{Reshape}(\text{AvgPool}(\mathbf{Linear}_{\mathbf{d} \to \mathbf{r}}(x)), (B, r))$$
 (12)

$$H(x) = (x_a \cdot W_g) + \text{StandardNormal}() \cdot \text{Softplus}(x_a \cdot W_{noise})$$
 (13)

where $W_g \in \mathbb{R}^{r \times n}$ and $W_{noise} \in \mathbb{R}^{r \times n}$ represent the trainable gating weight and the noise term, respectively. We select only the top k values on H(x) and set the rest to $-\infty$. After 'Softmax' operation, the gating scores G(x) can be calculated as follows:

$$G(x) = \text{Softmax}(\text{KeepTopK}(H(x), k))$$
 (14)

The role of the experts is to extract feature with multi-scale, which consist of Interpolate operation at a specific scale, $\mathrm{DWConv}_{3\times3}$ and $\mathrm{Upsample}$ operation to map the feature to the original scale. Let i-th expert be E_i with scale $s_i = \frac{1}{2^{i-1}}$, where i = 1, 2, 3, 4. The expert E_i processes the input x as follows:

$$E_i(x) = \text{UpSample}(\text{DWConv}_{3\times3}(\text{Interpolate}(\mathbf{Linear}_{\mathbf{d}\to\mathbf{r}}(x), s_i)))$$
 (15)

Finally, we obtain the output according to Eq. 1.

Multi-Scale An intuitive alternative is applying a multi-scale strategy, which utilizes n branches to extract features with different scales. The structural difference with M2oE is its lack of the gating network, as illustrated in Figure 9. The absence brings a higher parameter consumption, due to the fact that the gating network helps selectively activate sparse experts.

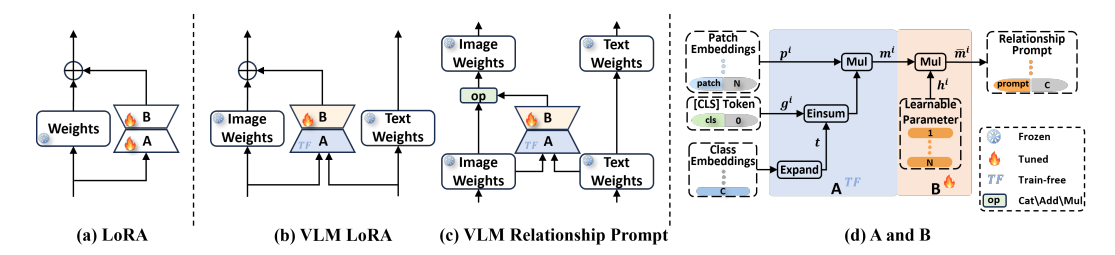


Figure 10: **Relationship prompt.** (a) LoRA. (b) VLM LoRA in a common-bypass mode. (c) VLM relationship prompt tuning. (d) Details of **A** and **B**. Note that **A** and **B** refer to ours IPT and APG.

C Motivation behind the design of RPM

The motivation behind the design of RPM is inspired by LoRA [58]. As illustrated in Figure 10 (a), considering that the main components of large models lie in a low intrinsic dimension, LoRA introduces dimensionality reduction matrix A and dimensionality enhancement matrix B into the bypass to fit the frozen weights. This approach enables fine-tuning the model with minimal training costs, thereby improving performance for specific tasks without changing the original parameters. Given that VLM has two branches to process image and text data, we initially adopt a common-bypass mode as shown in Figure 10 (b). The distinction between LoRA and VLM LoRA lies in the fact that matrix A in VLM LoRA accepts two types of modal inputs and it is training-free. It is important to note that we do not connect the output of matrix B with the embeddings from the text module for two reasons: their dimensions do not match and the relationship attention map from matrix A performs more effectively as a visual prompt rather than a textual prompt, as illustrated in Figure 1. However, the performance of implementing VLM LoRA was suboptimal. We discovered that a direct skip connection with the output of the current image weights that bypasses matrices A and B, achieves the same effect. Our analysis suggests that merely tuning the lightweight matrix B in a post-tuning model is found to be insufficient for adapting parameter-intensive weights. Consequently, we propose a prefix-tuning architecture as illustrated in Figure 10 (c). We position the two matrices between the preceding and current weights and established a skip connection with the original output of the preceding image weights rather than the current image weights. This circumvents the need to fit the parameter-intensive image weights. In light of this prefix-tuning architecture, we categorize this model into the category of prompt learning rather than adaptation, and thereby naming it relationship prompt learning. In addition, we consider three operations between the output of the preceding image weights and the output of matrix B: concatenation, addition, and Hadamard product. Following a quantitative analysis (shown in Table 14), we select the concatenation operation.

D More Details about Experiments

Zero-Shot Semantic Segmentation Setting We adopt the popular zero-shot setting as follows in [13, 9, 4, 3, 1, 31]. In the setting, we divide all classes into seen and unseen, only the seen classes are used in training. For the VOC dataset, we select 15 seen classes and 5 unseen classes, with the 'background' class excluded. For the COCO dataset, we divide all classes into 156 seen classes and 15 unseen classes. For the Context dataset, we select 50 seen classes (including 'background') and 10 unseen classes. These unseen classes are defined as follows:

Dataset	Unseen Classes
VOC	pottedplant, sheep, sofa, train, tymonitor
COCO	cow, giraffe, suitcase, frisbee, skateboard carrot, scissors, cardboard, clouds,
COCO	grass playingfield, river, road, tree, wall concrete
Context	cow, motorbike, sofa, cat, boat, fence bird, tv monitor, keyboard, aeroplane

Open-Vocabulary Semantic Segmentation Setting We employ the open-vocabulary setting as follows in [14, 12, 51, 53]. In this setting, we train our model on the COCO dataset and evaluate it on other datasets, including the VOC dataset with 20 classes (PAS-20), the Context dataset with 59 and 459 classes (PC-59 and PC-459), the ADE20K dataset with 150 and 847 classes (A-150 and A-847).

Text Prompt Templates For the VOC dataset, we apply a single template 'A photo of a {}'. For the Context and COCO dataset, we apply multiple templates as follows:

```
'A photo of a {}.' ; 'A photo of a small {}.' ; 'A photo of a medium {}.' ; 'A photo of a large {}.'

'This is a photo of a {}.' ; 'This is a photo of a small {}.' ; 'This is a photo of a medium {}.' ; 'This is a photo of a large {}.'

'A {} in the scene.' ; 'A photo of a {} in the scene.'

'There is a {} in the scene.' ; 'There is the {} in the scene.'

'This is a {} in the scene.' ; 'This is the {} in the scene.'
```

Full Experiment Results We show the full performance comparison of existing methods in the zero-shot and open-vocabulary semantic segmentation settings in Table 8 and Table 9.

Comparison with PEFT Methods We explore some parameter-efficient fine-tuning (PEFT) methods with baseline (i.e., the CLIP with LPM): 1) fine-tuning entire baseline; 2) only fine-tuning LPM; 3) BitFit [70], a sparse-fine-tuning method where only the bias-terms of the model (or a subset of them) are modified; 4) Adapter [71], which inserts a trainable adapter module between the transformer layers. 5) VPT [24], which inserts trainable tokens to the input feature of each transformer layer; 6) LST [72], which trains a ladder-side network, a small and separate network that takes intermediate activations as input via shortcut connections (called ladders) from the backbone networks and makes predictions. 7) SSF [73], which trains scale and shift parameters to modulate the visual features. 8) LoRA [58], which inserts a trainable dimensionality reduction matrix and a dimensionality enhancement matrix in parallel to the frozen weights. As illustrated in Table 10, our method shows significant improvements compared to PEFT methods. This is attributed to the fact that these PEFT methods only focus on how to train the baseline with fewer parameters, suitable only for image-level feature representation tasks, while our method not only trains the baseline with fewer parameters, but also focuses on applying capabilities suitable for image-level feature representation tasks directly to pixel-level semantic segmentation tasks. In summary, existing PEFT methods mainly focus on fine-tuning the task-specific model to improve performance on that task, while our method enables VLM to directly perform semantic segmentation.

Combination with VPT We explore the combination of our method and VPT in Table 11. When using VPT alone and in combination with our method, the number of trainable tokens in each layer is 400 and 40 respectively. Considering the impact of parameter initialization in VPT, the performance change after the combination is negligible.

Table 8: Full performance comparison in the zero-shot setting (unit:%). Here, the best results are shown in bold and the second-best results are underlined.

Methods		V	OC			CO	СО			Cor	text	
Methods	pAcc	$mIoU_s$	$mIoU_u$	hIoU	pAcc	$mIoU_s$	$mIoU_u$	hIoU	pAcc	$mIoU_s$	$mIoU_u$	hIoU
				w/o	self-tra							
SPNet [33]	-	78.0	15.6	26.1	-	35.2	8.7	14.0	-	-	-	-
ZS3Net [31]	-	77.3	17.7	28.7	-	34.7	9.5	15.0	52.8	20.8	12.7	15.8
CaGNet [30]	80.7	78.4	26.6	39.7	56.6	33.5	12.2	18.2	-	24.1	18.5	21.2
SIGN [28]	-	75.4	28.9	41.7	-	32.3	15.5	20.9	-	-	-	-
Joint [29]	-	77.7	32.5	45.9	-	-	-	-	-	33.0	14.9	20.5
ZegFormer [11]	-	86.4	63.6	73.3	-	36.6	33.2	34.8	-	-	-	-
ZegFormer+MAFT [51]	-	91.5	80.7	85.7	-	36.4	40.1	38.1	-	-	-	-
ZSSeg [12]	90.0	83.5	72.5	77.5	60.3	39.3	36.3	37.8	-	-	-	-
ZSSeg +MAFT [51]	-	87.1	76.1	81.2	-	36.1	35.9	36.0	-	-	-	-
ZegCLIP [19]	94.6	91.9	77.8	84.3	62.0	40.2	41.4	40.8	76.2	46.0	54.6	49.9
FreeSeg [10]		91.9	78.6	84.7		42.4	42.2	42.3		-		-
RPN(ours)	95.8	93.1	84.6	88.6	64.4	40.8	42.8	41.8	76.4	47.7	58.7	52.6
				w/	self-trai	ining						
SPNet [33]	-	77.8	25.8	38.8	-	34.6	26.9	30.3	-	-	-	-
ZS5Net [31]	-	78.0	21.2	33.3	-	34.9	10.6	16.2	49.5	27.0	20.7	23.4
CaGNet [30]	81.6	78.6	30.3	43.7	56.8	35.6	13.4	19.5	-	-	-	-
STRICT [34]	-	82.7	35.6	49.8	-	35.3	30.3	34.8	-	-	-	-
DiffMask [32]	-	71.4	65.0	68.1	-	-	-	-	-	-	-	-
ZSSeg [12]	88.7	79.2	78.1	79.3	63.8	39.6	43.6	41.5	-	-	-	-
ZegCLIP [19]	95.1	91.8	82.2	86.7	68.8	40.6	54.8	46.6	77.2	46.6	65.4	54.4
MaskCLIP† [8]	-	88.8	86.1	87.4	-	38.1	54.7	45.0	-	44.4	66.7	53.3
ZegCLIP [†] [19]	96.2	92.3	89.9	91.1	69.2	40.7	59.9	48.5	77.3	46.8	68.5	55.6
RPN†(ours)	97.1	93.1	93.6	93.3	69.3	<u>40.6</u>	61.2	48.8	78.3	48.1	70.8	57.3
				ful	ly super	vised						
ZegCLIP [19]	96.3	92.4	90.9	91.6	69.9	40.7	63.2	49.6	77.5	46.5	78.7	56.9
RPN(ours)	97.2	94.0	94.6	94.3	70.8	41.1	64.1	50.5	78.7	48.5	80.1	60.4

Table 9: **Full performance comparison in the open-vocabulary setting (unit:%).** Here, the best results are shown in bold and the second-best results are underlined.

Methods	VLM	Training Set	A-847	PC-459	A-150	PC-59	PAS-20
SPNet [33]	-	VOC	-	-	-	24.3	18.3
ZS3Net[31]	-	VOC	-	-	-	19.4	38.3
LSeg[59]	ViT-B/32	VOC-15	-	-	-	-	47.4
LSeg+[60]	ALIGN	COCO-Stuff	2.5	5.2	13.0	36.0	-
Han <i>et al</i> .[61]	ViT-B/16	COCO Panoptic [62]	3.5	7.1	18.8	45.2	83.2
GroupViT[63]	ViT-S/16	GCC[64]+YFCC[65]	4.3	4.9	10.6	25.9	50.7
ZegFormer[11]	ViT-B/16	COCO-Stuff	5.6	10.4	18.0	45.5	89.5
OpenSeg [60]	ALIGN	COCO Panoptic+Loc. Narr.[66]	4.4	7.9	17.5	40.1	-
FreeSeg [10]	-	COCO-Stuff	7.1	6.4	17.9	34.4	85.6
FreeSeg+MAFT [51]	-	COCO-Stuff	10.1	12.8	29.1	53.5	90.0
OVSeg [14]	ViT-B/16	COCO-Stuff+COCO Caption	7.1	11.0	24.8	53.3	92.6
CAT-Seg[52]	ViT-B/16	COCO-Stuff	8.4	16.6	27.2	57.5	93.7
SAN[53]	ViT-B/16	COCO-Stuff	10.1	12.6	27.5	53.8	94.0
SED[54]	ConvNeXt-B	COCO-Stuff	11.4	18.6	31.6	57.3	94.4
RPN(ours)	ViT-B/16	COCO-Stuff	11.4	<u>17.3</u>	<u>31.5</u>	57.1	95.2
LSeg[59]	ViT-B/32	VOC-15	-	-	-	-	52.3
OpenSeg [60]	ALIGN	COCO Panoptic+Loc. Narr.	8.1	11.5	26.4	44.8	-
OVSeg [14]	ViT-L/14	COCO-Stuff+COCO Caption	9.0	12.4	29.6	55.7	94.5
Ding <i>et al</i> .[67]	ViT-L/14	COCO Panoptic	8.2	10.0	23.7	45.9	-
ODISE[68]	ViT-L/14	COCO Panoptic	11.1	14.5	29.9	57.3	-
HIPIE[69]	BERT-B	COCO Panoptic	-	-	29.0	59.3	-
CAT-Seg[52]	ViT-L/14	COCO-Stuff	10.8	20.4	31.5	62.0	96.6
SAN[53]	ViT-L/14	COCO-Stuff	13.7	17.1	33.3	60.2	95.5
FC-CLIP[55]	ConvNeXt-L	COCO Panoptic	14.8	18.2	34.1	58.4	95.4
SED[54]	ConvNeXt-L	COCO-Stuff	13.9	22.6	<u>35.2</u>	60.6	96.1
RPN(ours)	ViT-L/14	COCO-Stuff	14.9	<u>22.1</u>	36.4	<u>61.9</u>	<u>96.6</u>

Table 10: **Performance comparison with PEFT methods (unit:%).** Baseline represents the CLIP model with LPM. **#Params(M)** represents the number of trainable parameters during training.

Methods	#Params(M)		V	OC		COCO				
Methous	π1 al alli5(1V1)	pAcc	$mIoU_s$	\mathbf{mIoU}_u	hIoU	pAcc	\mathbf{mIoU}_s	\mathbf{mIoU}_u	hIoU	
Baseline	154.5	84.1	83.5	31.2	45.4	47.8	30.1	19.6	23.7	
LPM-only	0.8	88.8	87.3	45.3	59.6	49.3	31.3	20.3	24.6	
BitFit[70]	4.0	89.7	79.3	51.2	62.2	50.6	35.6	23.3	28.2	
Adapter[71]	3.9	90.3	79.7	51.6	62.6	51.4	36.0	24.1	28.9	
VPT[24]	4.0	90.9	81.0	52.9	64.0	51.9	37.5	25.9	30.6	
LST[72]	11.5	88.6	78.7	50.4	61.4	50.1	34.8	22.6	27.4	
SSF[73]	4.4	90.8	80.8	52.7	63.8	51.7	37.3	25.6	30.4	
LoRA[58]	4.0	91.3	82.2	53.1	64.5	52.9	38.7	27.0	31.8	
RPN(ours)	3.2	95.8	93.1	84.6	88.6	64.4	40.8	42.8	41.8	

Table 11: **Performance of combining our method and VPT (unit:%). #Params(M)** represents the number of trainable parameters during training.

Methods	#Params(M)		V(OC		COCO				
Methous	π1 a1 a1115(1V1)	pAcc	\mathbf{mIoU}_s	\mathbf{mIoU}_u	hIoU	pAcc	\mathbf{mIoU}_s	\mathbf{mIoU}_u	hIoU	
VPT[24]	4.0	90.9	81.0	52.9	64.0	51.9	37.5	25.9	30.6	
RPN(ours)	3.2	95.8	93.1	84.6	88.6	64.4	40.8	42.8	41.8	
RPN+VPT	3.6	95.8	93.1	84.2	88.4	64.4	40.3	43.1	41.7	

Table 12: Impact of different pre-trained weights for the plain encoder (unit:%).

Weights	VOC				COCO			
	pAcc	\mathbf{mIoU}_s	\mathbf{mIoU}_u	hIoU	pAcc	\mathbf{mIoU}_s	\mathbf{mIoU}_u	hIoU
ViT[56]	85.9	81.0	42.9	56.1	46.7	29.3	19.9	23.7
MAE[74]	87.1	82.4	43.7	57.1	48.2	30.8	21.5	25.3
CLIP[5]	95.8	93.1	84.6	88.6	64.4	40.8	42.8	41.8

Table 13: **Impact of RPM in different layers (unit:%).** 'Number' represent the number of layer at which RPM is applied. Note that 'all' do not include the last layer.

Datasets	Number	pAcc	\mathbf{mIoU}_s	\mathbf{mIoU}_u	hIoU
	1	93.1	88.4	74.1	80.6
	11	92.8	88.7	70.3	78.4
VOC	{1,3,5,7,9,11}	93.9	89.4	80.9	84.9
	{2,4,6,8,10}	93.9	89.1	80.1	84.4
	all	95.8	93.1	84.6	88.6
COCO	1	60.2	39.8	35.8	37.7
	11	60.1	39.4	33.6	36.3
	{1,3,5,7,9,11}	61.9	40.2	38.5	39.3
	{2,4,6,8,10}	61.9	40.1	38.4	39.2
	all	64.4	40.8	42.8	41.8

Table 14: Ablation study on three kinds of prefix-tuning operations (unit: %).

Datasets	Mul	Add	Cat	pAcc	\mathbf{mIoU}_s	\mathbf{mIoU}_u	hIoU
	√			88.8	87.3	45.3	59.6
VOC		\checkmark		90.3	83.2	69.5	75.7
			\checkmark	95.8	93.1	84.6	88.6
	√			49.3	31.3	20.3	24.6
COCO		\checkmark		56.8	36.6	25.7	30.2
			\checkmark	64.4	40.8	42.8	41.8

Impact of Different Pre-trained Weights for the Plain Encoder We explore different pre-trained weights of the plain encoder in Table 12. These weights are from supervised learning, unsupervised learning and weakly-supervised learning of text signals. ViT [56] applies supervised learning to learn visual representation. MAE [74] applies self-supervised learning to learn rich semantics. The two methods learn uni-modal knowledge. CLIP[5] applies text as a supervisory signal and adopts contrastive learning to learn general visual representation. It is a multi-modal learning method. The results show that our method has limitations in mining uni-modal visual knowledge. In addition, compared to ViT and MAE, CLIP uses more data to pre-train the plain encoder. This also shows that even though our method is superior, it still cannot get rid of the dependence on a large amount of data.

Impact of RPM in Different Layers We adopt a layer-by-layer guidance mode (i.e., all) as shown in Table 13. Our method is evaluated across various network depths, including shallow layers, deep layers, and interval layer mode. We find that the performance of single-layer mode (such as layers 1 or 11) are significantly worse than those of multi-layer modes. The layer-by-layer mode demonstrates optimal performance on both the VOC and COCO datasets.

Impact of Different Prefix-tuning Operations We compare three prefix-tuning operations as shown in Figure 10 (c): concatenation, addition, and Hadamard product. Results from Table 14 indicate that the relationship prompt should not directly modify the original feature (like addition or Hadamard product), but rather should influence the model indirectly by computing the attention between the prompt and the original feature (like concatenation).

E Visualization

Baseline represents the frozen CLIP model with LPM.



Figure 11: Qualitative analysis. The unseen classes include tree, frisbee, grass and road.

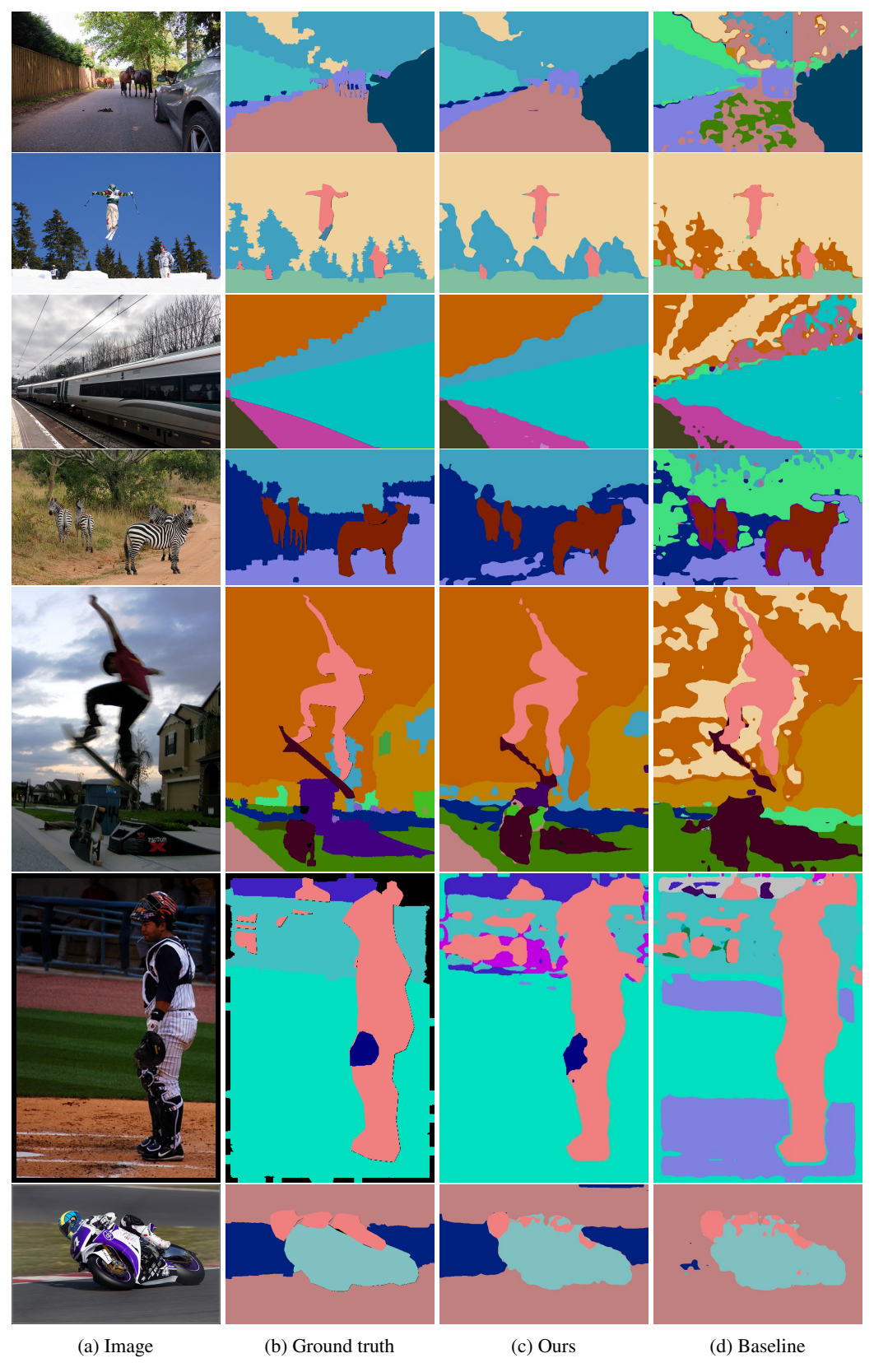


Figure 12: **Qualitative analysis.** The unseen classes include tree, clouds, skateboard, playingfield, wall-concrete, grass and road.

NeurIPS Paper Checklist

1. Claims

Question: Do the main claims made in the abstract and introduction accurately reflect the paper's contributions and scope?

Answer: [Yes]

Justification: We summarize our contributions and scope in the abstract and introduction.

Guidelines:

- The answer NA means that the abstract and introduction do not include the claims made in the paper.
- The abstract and/or introduction should clearly state the claims made, including the contributions made in the paper and important assumptions and limitations. A No or NA answer to this question will not be perceived well by the reviewers.
- The claims made should match theoretical and experimental results, and reflect how much the results can be expected to generalize to other settings.
- It is fine to include aspirational goals as motivation as long as it is clear that these goals are not attained by the paper.

2. Limitations

Question: Does the paper discuss the limitations of the work performed by the authors?

Answer: [Yes]

Justification: We show that even if our method is superior, it still cannot get rid of the dependence on a large amount of data in Appnedix D.

Guidelines:

- The answer NA means that the paper has no limitation while the answer No means that the paper has limitations, but those are not discussed in the paper.
- The authors are encouraged to create a separate "Limitations" section in their paper.
- The paper should point out any strong assumptions and how robust the results are to violations of these assumptions (e.g., independence assumptions, noiseless settings, model well-specification, asymptotic approximations only holding locally). The authors should reflect on how these assumptions might be violated in practice and what the implications would be.
- The authors should reflect on the scope of the claims made, e.g., if the approach was only tested on a few datasets or with a few runs. In general, empirical results often depend on implicit assumptions, which should be articulated.
- The authors should reflect on the factors that influence the performance of the approach. For example, a facial recognition algorithm may perform poorly when image resolution is low or images are taken in low lighting. Or a speech-to-text system might not be used reliably to provide closed captions for online lectures because it fails to handle technical jargon.
- The authors should discuss the computational efficiency of the proposed algorithms and how they scale with dataset size.
- If applicable, the authors should discuss possible limitations of their approach to address problems of privacy and fairness.
- While the authors might fear that complete honesty about limitations might be used by reviewers as grounds for rejection, a worse outcome might be that reviewers discover limitations that aren't acknowledged in the paper. The authors should use their best judgment and recognize that individual actions in favor of transparency play an important role in developing norms that preserve the integrity of the community. Reviewers will be specifically instructed to not penalize honesty concerning limitations.

3. Theory Assumptions and Proofs

Question: For each theoretical result, does the paper provide the full set of assumptions and a complete (and correct) proof?

Answer: [Yes]

Justification: We provide the full set of assumptions and a complete (and correct) proof. Guidelines:

- The answer NA means that the paper does not include theoretical results.
- All the theorems, formulas, and proofs in the paper should be numbered and crossreferenced.
- All assumptions should be clearly stated or referenced in the statement of any theorems.
- The proofs can either appear in the main paper or the supplemental material, but if they appear in the supplemental material, the authors are encouraged to provide a short proof sketch to provide intuition.
- Inversely, any informal proof provided in the core of the paper should be complemented by formal proofs provided in appendix or supplemental material.
- Theorems and Lemmas that the proof relies upon should be properly referenced.

4. Experimental Result Reproducibility

Question: Does the paper fully disclose all the information needed to reproduce the main experimental results of the paper to the extent that it affects the main claims and/or conclusions of the paper (regardless of whether the code and data are provided or not)?

Answer: [Yes]

Justification: We provide details of our settings in the paper.

Guidelines:

- The answer NA means that the paper does not include experiments.
- If the paper includes experiments, a No answer to this question will not be perceived
 well by the reviewers: Making the paper reproducible is important, regardless of
 whether the code and data are provided or not.
- If the contribution is a dataset and/or model, the authors should describe the steps taken to make their results reproducible or verifiable.
- Depending on the contribution, reproducibility can be accomplished in various ways. For example, if the contribution is a novel architecture, describing the architecture fully might suffice, or if the contribution is a specific model and empirical evaluation, it may be necessary to either make it possible for others to replicate the model with the same dataset, or provide access to the model. In general, releasing code and data is often one good way to accomplish this, but reproducibility can also be provided via detailed instructions for how to replicate the results, access to a hosted model (e.g., in the case of a large language model), releasing of a model checkpoint, or other means that are appropriate to the research performed.
- While NeurIPS does not require releasing code, the conference does require all submissions to provide some reasonable avenue for reproducibility, which may depend on the nature of the contribution. For example
- (a) If the contribution is primarily a new algorithm, the paper should make it clear how to reproduce that algorithm.
- (b) If the contribution is primarily a new model architecture, the paper should describe the architecture clearly and fully.
- (c) If the contribution is a new model (e.g., a large language model), then there should either be a way to access this model for reproducing the results or a way to reproduce the model (e.g., with an open-source dataset or instructions for how to construct the dataset).
- (d) We recognize that reproducibility may be tricky in some cases, in which case authors are welcome to describe the particular way they provide for reproducibility. In the case of closed-source models, it may be that access to the model is limited in some way (e.g., to registered users), but it should be possible for other researchers to have some path to reproducing or verifying the results.

5. Open access to data and code

Question: Does the paper provide open access to the data and code, with sufficient instructions to faithfully reproduce the main experimental results, as described in supplemental material?

Answer: [Yes]

Justification: We provide an anonymous URL in the supplementary material.

Guidelines:

- The answer NA means that paper does not include experiments requiring code.
- Please see the NeurIPS code and data submission guidelines (https://nips.cc/ public/guides/CodeSubmissionPolicy) for more details.
- While we encourage the release of code and data, we understand that this might not be possible, so "No" is an acceptable answer. Papers cannot be rejected simply for not including code, unless this is central to the contribution (e.g., for a new open-source benchmark).
- The instructions should contain the exact command and environment needed to run to reproduce the results. See the NeurIPS code and data submission guidelines (https: //nips.cc/public/guides/CodeSubmissionPolicy) for more details.
- · The authors should provide instructions on data access and preparation, including how to access the raw data, preprocessed data, intermediate data, and generated data, etc.
- The authors should provide scripts to reproduce all experimental results for the new proposed method and baselines. If only a subset of experiments are reproducible, they should state which ones are omitted from the script and why.
- At submission time, to preserve anonymity, the authors should release anonymized versions (if applicable).
- Providing as much information as possible in supplemental material (appended to the paper) is recommended, but including URLs to data and code is permitted.

6. Experimental Setting/Details

Question: Does the paper specify all the training and test details (e.g., data splits, hyperparameters, how they were chosen, type of optimizer, etc.) necessary to understand the results?

Answer: [Yes]

Justification: We provide details of our settings in the paper.

Guidelines:

- The answer NA means that the paper does not include experiments.
- The experimental setting should be presented in the core of the paper to a level of detail that is necessary to appreciate the results and make sense of them.
- The full details can be provided either with the code, in appendix, or as supplemental material.

7. Experiment Statistical Significance

Question: Does the paper report error bars suitably and correctly defined or other appropriate information about the statistical significance of the experiments?

Answer: [Yes]

Justification: We report error bars suitably and correctly defined or other appropriate information about the statistical significance of the experiments.

- The answer NA means that the paper does not include experiments.
- The authors should answer "Yes" if the results are accompanied by error bars, confidence intervals, or statistical significance tests, at least for the experiments that support the main claims of the paper.
- The factors of variability that the error bars are capturing should be clearly stated (for example, train/test split, initialization, random drawing of some parameter, or overall run with given experimental conditions).
- The method for calculating the error bars should be explained (closed form formula, call to a library function, bootstrap, etc.)
- The assumptions made should be given (e.g., Normally distributed errors).

- It should be clear whether the error bar is the standard deviation or the standard error
 of the mean.
- It is OK to report 1-sigma error bars, but one should state it. The authors should preferably report a 2-sigma error bar than state that they have a 96% CI, if the hypothesis of Normality of errors is not verified.
- For asymmetric distributions, the authors should be careful not to show in tables or figures symmetric error bars that would yield results that are out of range (e.g. negative error rates).
- If error bars are reported in tables or plots, The authors should explain in the text how they were calculated and reference the corresponding figures or tables in the text.

8. Experiments Compute Resources

Question: For each experiment, does the paper provide sufficient information on the computer resources (type of compute workers, memory, time of execution) needed to reproduce the experiments?

Answer: [Yes]

Justification: We provide theses information in our paper.

Guidelines:

- The answer NA means that the paper does not include experiments.
- The paper should indicate the type of compute workers CPU or GPU, internal cluster, or cloud provider, including relevant memory and storage.
- The paper should provide the amount of compute required for each of the individual experimental runs as well as estimate the total compute.
- The paper should disclose whether the full research project required more compute than the experiments reported in the paper (e.g., preliminary or failed experiments that didn't make it into the paper).

9. Code Of Ethics

Question: Does the research conducted in the paper conform, in every respect, with the NeurIPS Code of Ethics https://neurips.cc/public/EthicsGuidelines?

Answer: [Yes]
Justification: Yes.

Guidelines:

- The answer NA means that the authors have not reviewed the NeurIPS Code of Ethics.
- If the authors answer No, they should explain the special circumstances that require a deviation from the Code of Ethics.
- The authors should make sure to preserve anonymity (e.g., if there is a special consideration due to laws or regulations in their jurisdiction).

10. Broader Impacts

Question: Does the paper discuss both potential positive societal impacts and negative societal impacts of the work performed?

Answer: [NA]

Justification: Our paper belongs to foundational research.

- The answer NA means that there is no societal impact of the work performed.
- If the authors answer NA or No, they should explain why their work has no societal impact or why the paper does not address societal impact.
- Examples of negative societal impacts include potential malicious or unintended uses (e.g., disinformation, generating fake profiles, surveillance), fairness considerations (e.g., deployment of technologies that could make decisions that unfairly impact specific groups), privacy considerations, and security considerations.

- The conference expects that many papers will be foundational research and not tied to particular applications, let alone deployments. However, if there is a direct path to any negative applications, the authors should point it out. For example, it is legitimate to point out that an improvement in the quality of generative models could be used to generate deepfakes for disinformation. On the other hand, it is not needed to point out that a generic algorithm for optimizing neural networks could enable people to train models that generate Deepfakes faster.
- The authors should consider possible harms that could arise when the technology is being used as intended and functioning correctly, harms that could arise when the technology is being used as intended but gives incorrect results, and harms following from (intentional or unintentional) misuse of the technology.
- If there are negative societal impacts, the authors could also discuss possible mitigation strategies (e.g., gated release of models, providing defenses in addition to attacks, mechanisms for monitoring misuse, mechanisms to monitor how a system learns from feedback over time, improving the efficiency and accessibility of ML).

11. Safeguards

Question: Does the paper describe safeguards that have been put in place for responsible release of data or models that have a high risk for misuse (e.g., pretrained language models, image generators, or scraped datasets)?

Answer: [NA]

Justification: Our paper belongs to foundational research.

Guidelines:

- The answer NA means that the paper poses no such risks.
- Released models that have a high risk for misuse or dual-use should be released with necessary safeguards to allow for controlled use of the model, for example by requiring that users adhere to usage guidelines or restrictions to access the model or implementing safety filters.
- Datasets that have been scraped from the Internet could pose safety risks. The authors should describe how they avoided releasing unsafe images.
- We recognize that providing effective safeguards is challenging, and many papers do
 not require this, but we encourage authors to take this into account and make a best
 faith effort.

12. Licenses for existing assets

Question: Are the creators or original owners of assets (e.g., code, data, models), used in the paper, properly credited and are the license and terms of use explicitly mentioned and properly respected?

Answer: [Yes]

Justification: They are properly credited and respected.

- The answer NA means that the paper does not use existing assets.
- The authors should cite the original paper that produced the code package or dataset.
- The authors should state which version of the asset is used and, if possible, include a URL.
- The name of the license (e.g., CC-BY 4.0) should be included for each asset.
- For scraped data from a particular source (e.g., website), the copyright and terms of service of that source should be provided.
- If assets are released, the license, copyright information, and terms of use in the package should be provided. For popular datasets, paperswithcode.com/datasets has curated licenses for some datasets. Their licensing guide can help determine the license of a dataset.
- For existing datasets that are re-packaged, both the original license and the license of the derived asset (if it has changed) should be provided.

 If this information is not available online, the authors are encouraged to reach out to the asset's creators.

13. New Assets

Question: Are new assets introduced in the paper well documented and is the documentation provided alongside the assets?

Answer: [NA]

Justification: We do not release new assets.

Guidelines:

- The answer NA means that the paper does not release new assets.
- Researchers should communicate the details of the dataset/code/model as part of their submissions via structured templates. This includes details about training, license, limitations, etc.
- The paper should discuss whether and how consent was obtained from people whose asset is used.
- At submission time, remember to anonymize your assets (if applicable). You can either create an anonymized URL or include an anonymized zip file.

14. Crowdsourcing and Research with Human Subjects

Question: For crowdsourcing experiments and research with human subjects, does the paper include the full text of instructions given to participants and screenshots, if applicable, as well as details about compensation (if any)?

Answer: [NA]

Justification: We do not involve crowdsourcing nor research with human subjects.

Guidelines:

- The answer NA means that the paper does not involve crowdsourcing nor research with human subjects.
- Including this information in the supplemental material is fine, but if the main contribution of the paper involves human subjects, then as much detail as possible should be included in the main paper.
- According to the NeurIPS Code of Ethics, workers involved in data collection, curation, or other labor should be paid at least the minimum wage in the country of the data collector.

15. Institutional Review Board (IRB) Approvals or Equivalent for Research with Human Subjects

Question: Does the paper describe potential risks incurred by study participants, whether such risks were disclosed to the subjects, and whether Institutional Review Board (IRB) approvals (or an equivalent approval/review based on the requirements of your country or institution) were obtained?

Answer: [NA]

Justification: We do not involve crowdsourcing nor research with human subjects.

- The answer NA means that the paper does not involve crowdsourcing nor research with human subjects.
- Depending on the country in which research is conducted, IRB approval (or equivalent) may be required for any human subjects research. If you obtained IRB approval, you should clearly state this in the paper.
- We recognize that the procedures for this may vary significantly between institutions and locations, and we expect authors to adhere to the NeurIPS Code of Ethics and the guidelines for their institution.
- For initial submissions, do not include any information that would break anonymity (if applicable), such as the institution conducting the review.